

Fermilab Joint Experimental-Theoretical Seminar
Fermilab, February 5, 2010

Shedding light on the Higgs: diphoton cross section measurements at DØ

Aurelio Juste

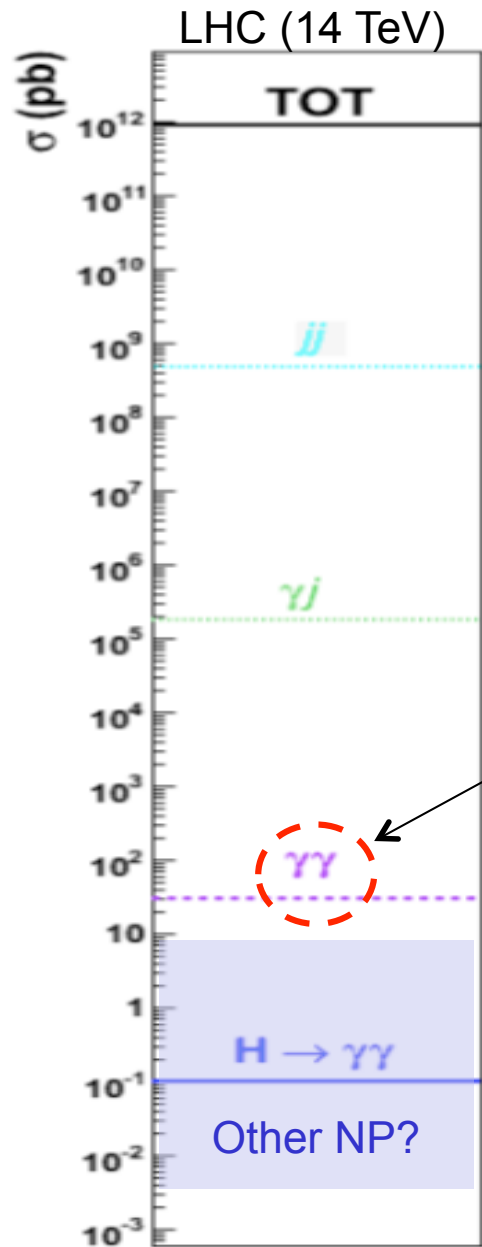
Fermilab, ICREA/IFAE (Barcelona)

For the DØ Collaboration

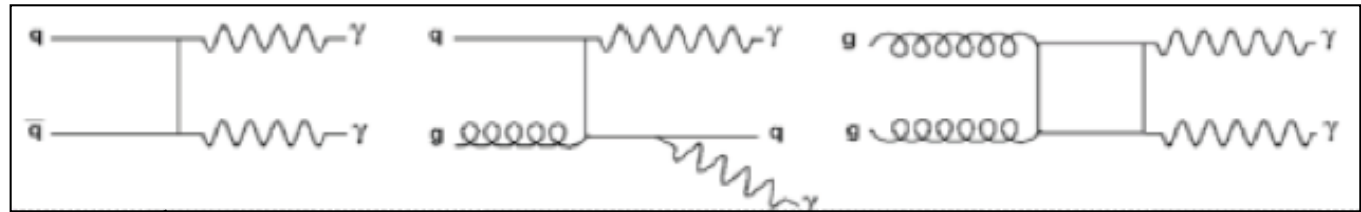
Outline

- Motivation
- Theoretical overview
- Experimental analysis
 - Photon identification
 - Event selection
 - Ingredients for differential cross section measurement
- Measurements and comparison with theory
- Summary and conclusions

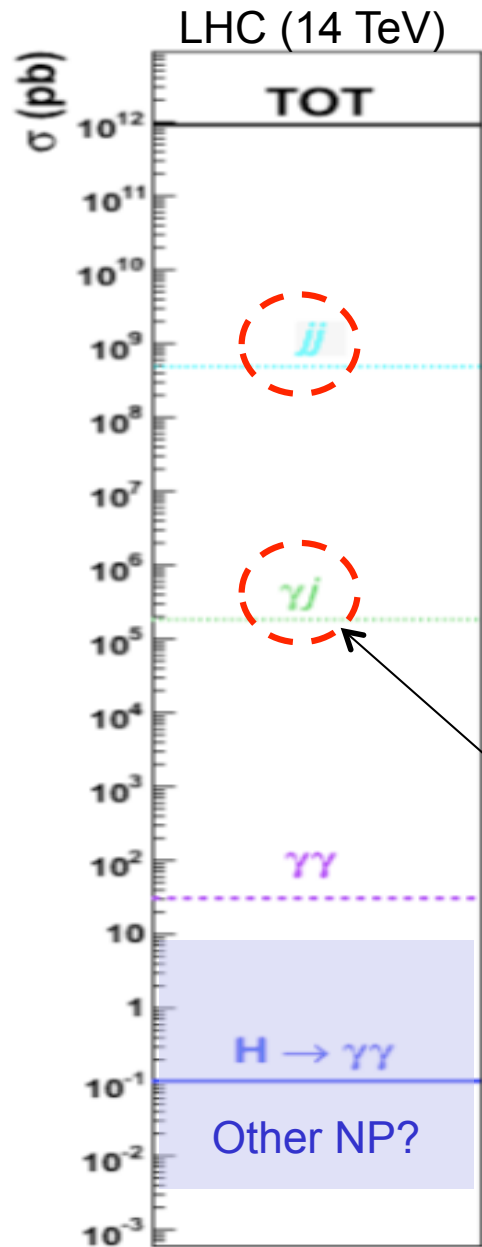
Prompt diphoton production at hadron colliders



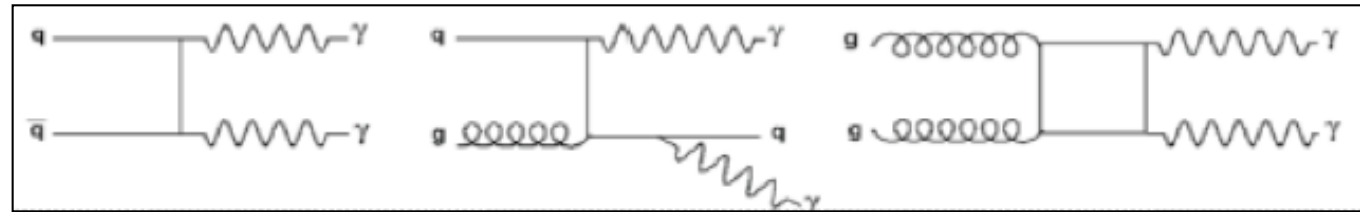
- **Prompt photons** = photons produced directly in perturbative scattering or via parton fragmentation (as opposed to non-perturbative photon production in meson decays).
- Main source of prompt diphoton production at hadron colliders via QCD interactions.



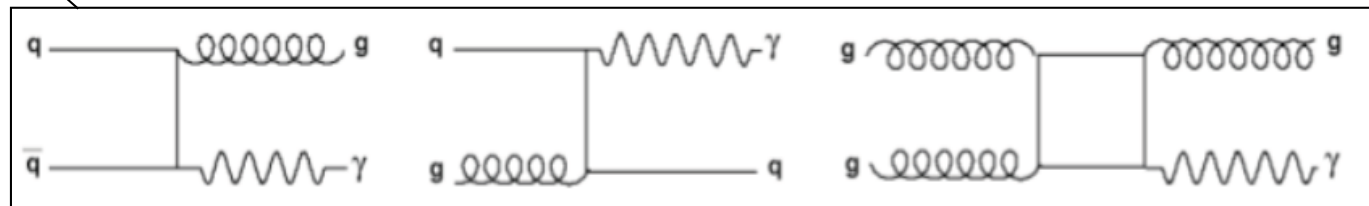
Prompt diphoton production at hadron colliders



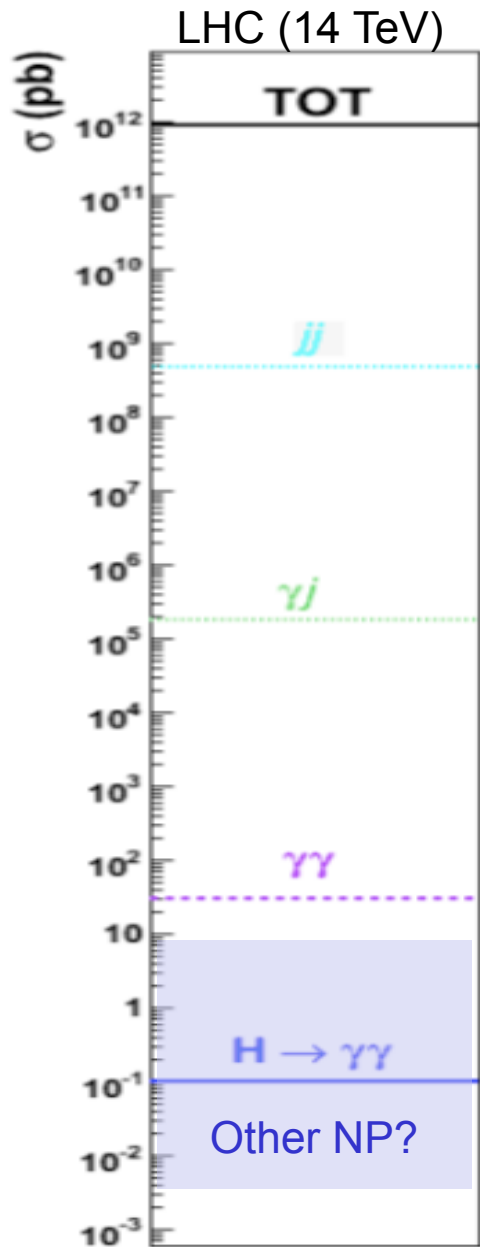
- **Prompt photons** = photons produced directly in perturbative scattering or via parton fragmentation (as opposed to non-perturbative photon production in meson decays).
- Main source of prompt diphoton production at hadron colliders via QCD interactions.



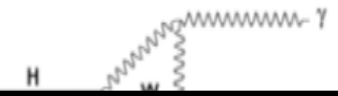
- **Main background: γ +jet and dijet**, with one or two jets misidentified as photons \rightarrow reducible background.



Prompt diphoton production at hadron colliders



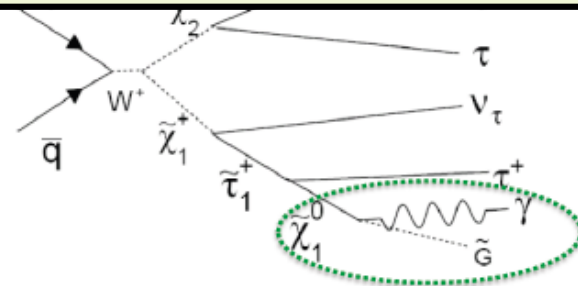
- **Prompt photons** = photons produced directly in perturbative scattering or via parton fragmentation (as opposed to non-perturbative photon production in meson decays).
- At much smaller rate, prompt diphotons may originate from more exotic (and exciting!) production mechanisms:
 - Higgs decay



Precise measurements of QCD $\gamma\gamma$ production should puts us on solid footing to search for new physics:

- Validate/improve theoretical predictions for irreducible (QCD $\gamma\gamma$) background.
- Develop/demonstrate good control over reducible backgrounds.

- SUSY
- ...

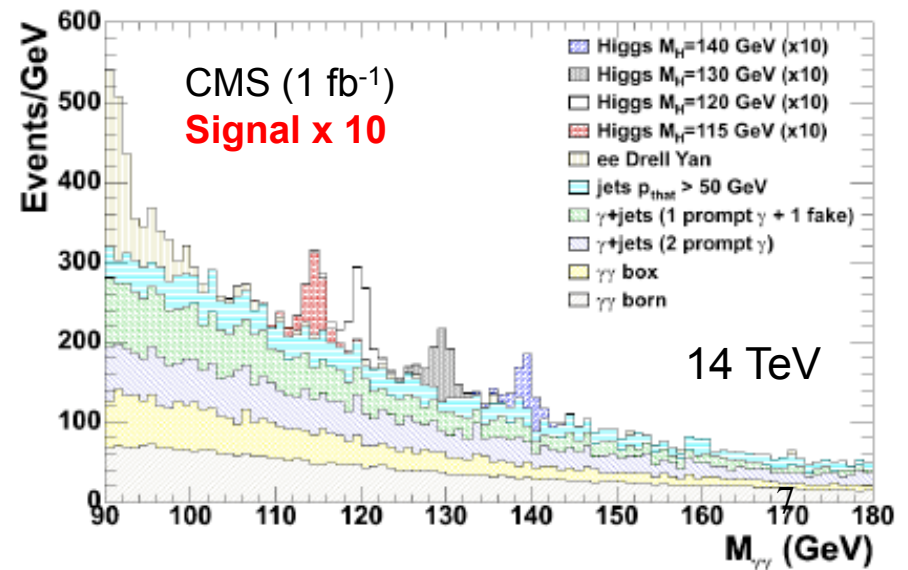
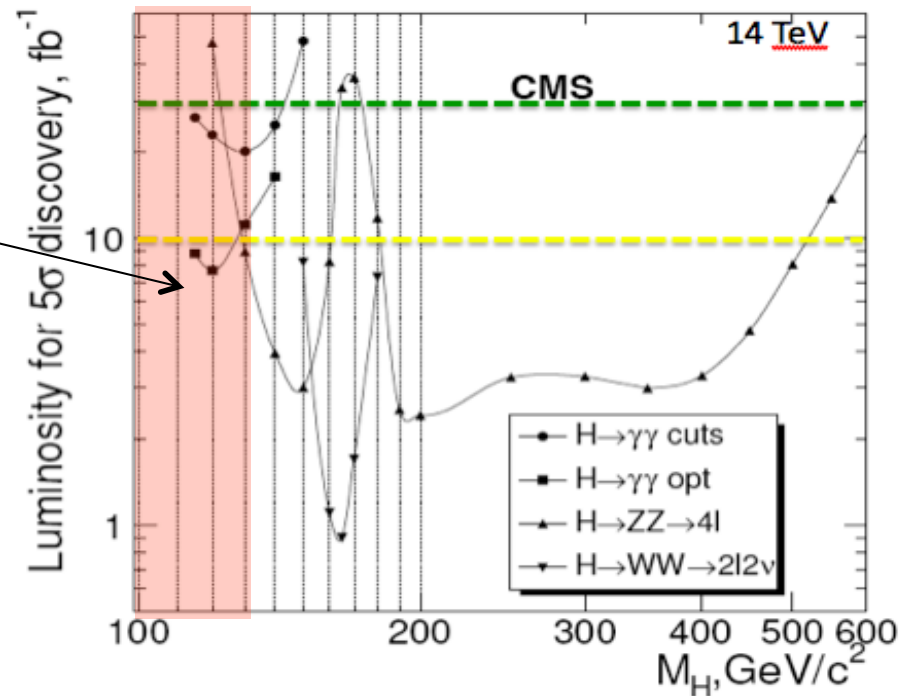


H $\rightarrow\gamma\gamma$ at the LHC

H $\rightarrow\gamma\gamma$ currently main discovery channel for $m_H < 130$ GeV.

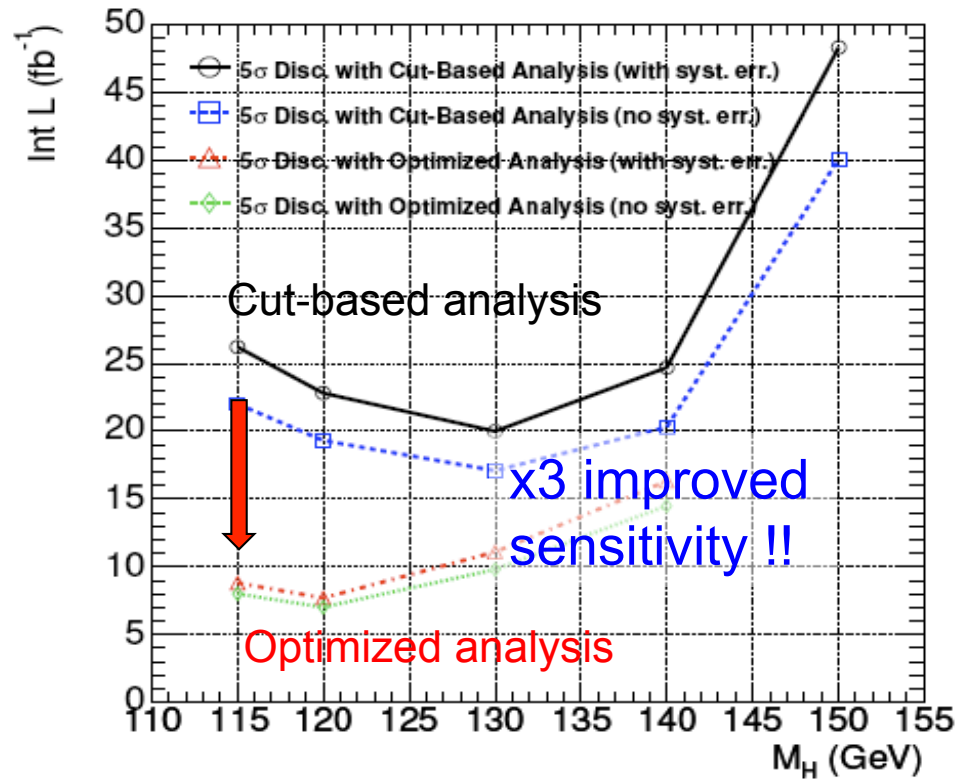
Inclusive analysis:

- 2 isolated high p_T photons
- Look for bump in $M_{\gamma\gamma}$ on top of steeply falling background.
- Very challenging: small S/B. Needs:
 - Excellent photon ID
 - Best possible energy resolution
- Background predicted from sidebands in data.
- Required luminosity for 5σ discovery at $m_H=115$ GeV: 26 fb^{-1} (CMS).

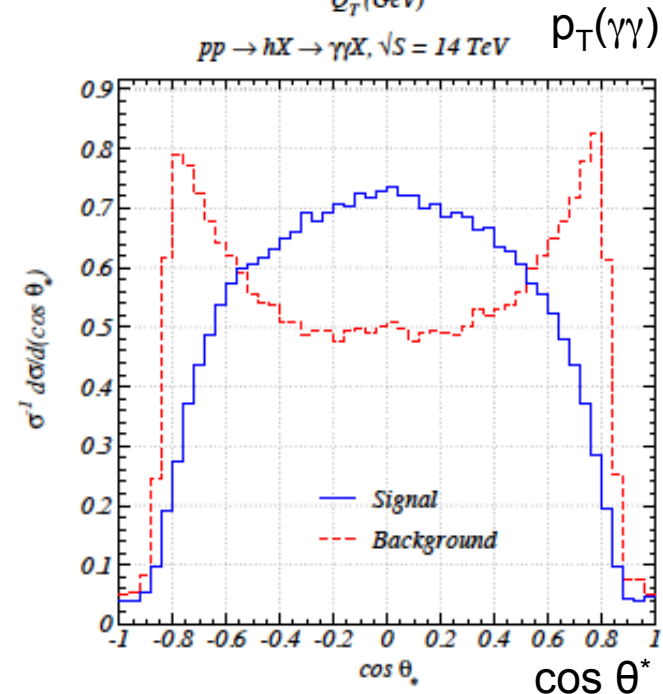
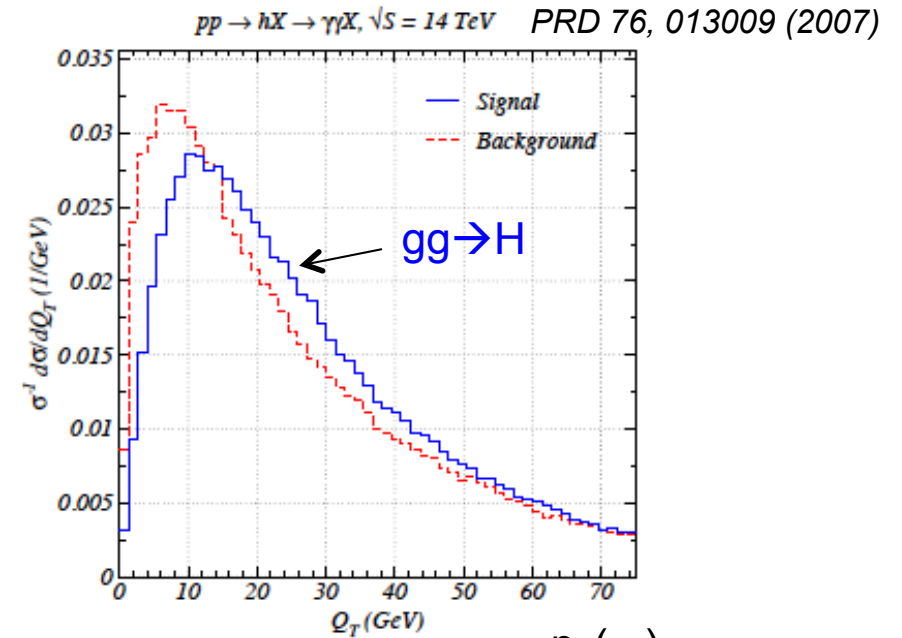


H $\rightarrow\gamma\gamma$ at the LHC

- Optimize analysis by exploiting additional discriminant variables:

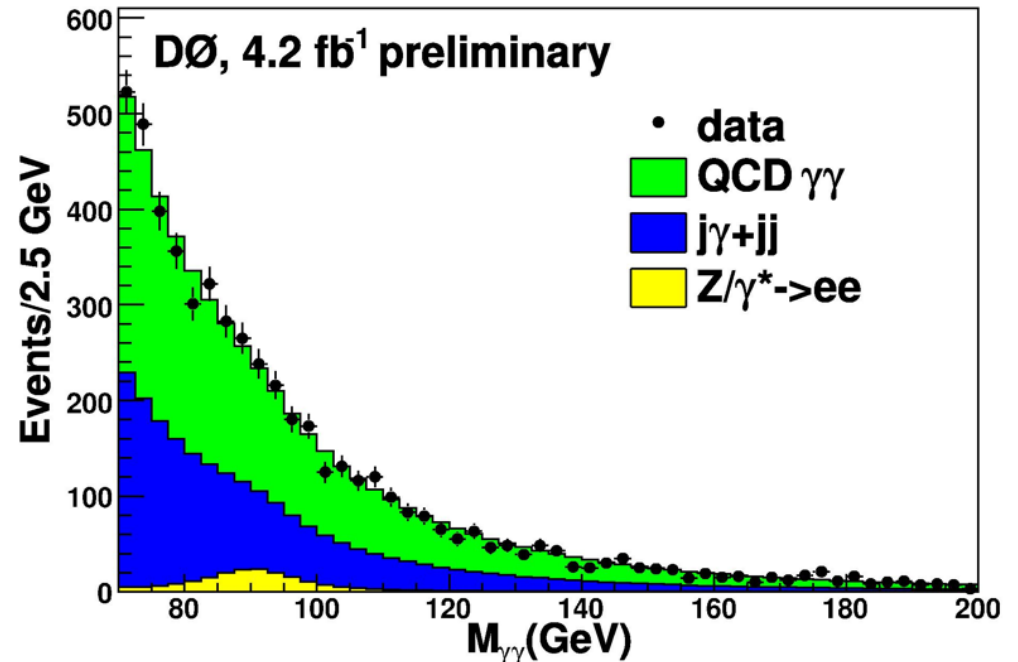


Should benefit from a precise theoretical prediction for irreducible background



What about $H \rightarrow \gamma\gamma$ at the Tevatron?

- Very small SM production rate: ~ 3 fb at $M_H = 115$ GeV.
 - Even with 10 fb^{-1} /experiment, no observation expected at the Tevatron.
 - However, this channel contributes to SM Higgs sensitivity in the difficult intermediate mass region ~ 125 GeV.
- Event selection:
2 photons with $p_T > 25$ GeV and $|\eta| < 1.1$
- Use diphoton mass spectrum
- Background estimated from data:
 - $\gamma+j$ and dijet ($\sim 40\%$)
 - Direct QCD $\gamma\gamma$ ($\sim 60\%$) via sideband fitting.



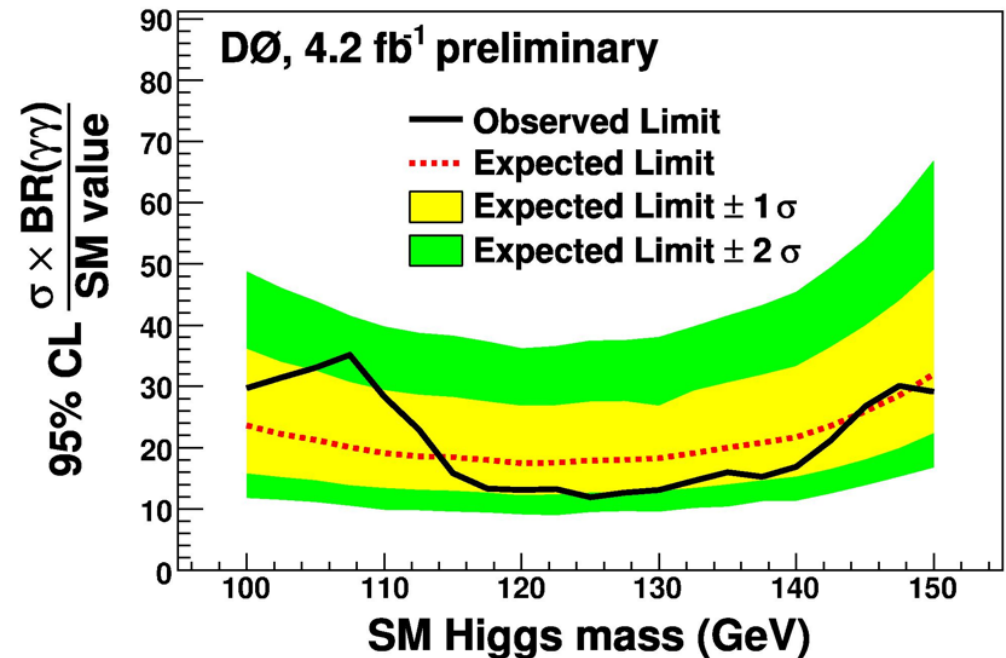
What about $H \rightarrow \gamma\gamma$ at the Tevatron?

- Very small SM production rate: ~ 3 fb at $M_H = 115$ GeV.
 - Even with 10 fb^{-1} /experiment, no observation expected at the Tevatron.
 - However, this channel contributes to SM Higgs sensitivity in the difficult intermediate mass region ~ 125 GeV.
- Event selection:
2 photons with $p_T > 25$ GeV and $|\eta| < 1.1$
- Use diphoton mass spectrum.
- Background estimated from data:
 - $\gamma+j$ and dijet ($\sim 40\%$)
 - Direct QCD $\gamma\gamma$ ($\sim 60\%$) via sideband fitting.

At $m_H = 115$ GeV:

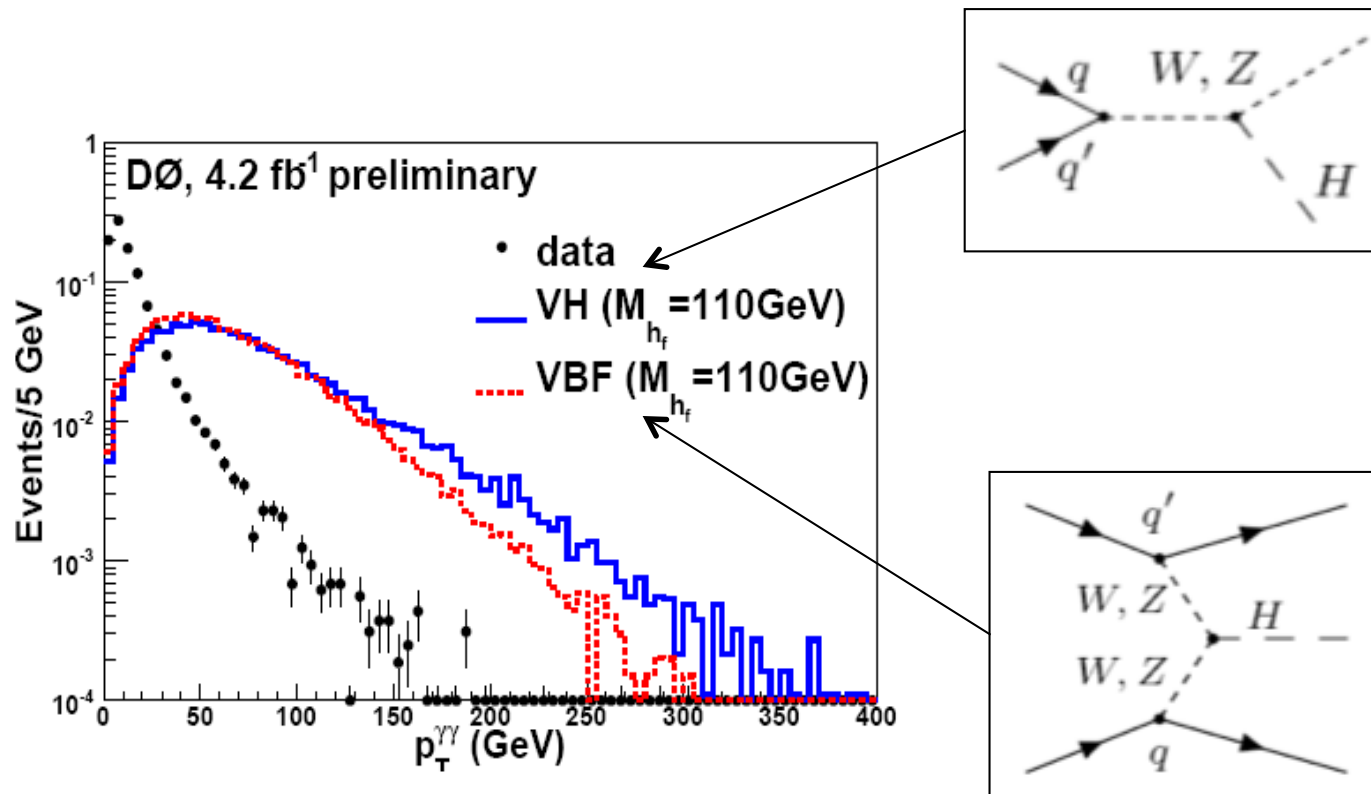
Expected limit: 18.5 x SM

Observed limit: 15.8 x SM



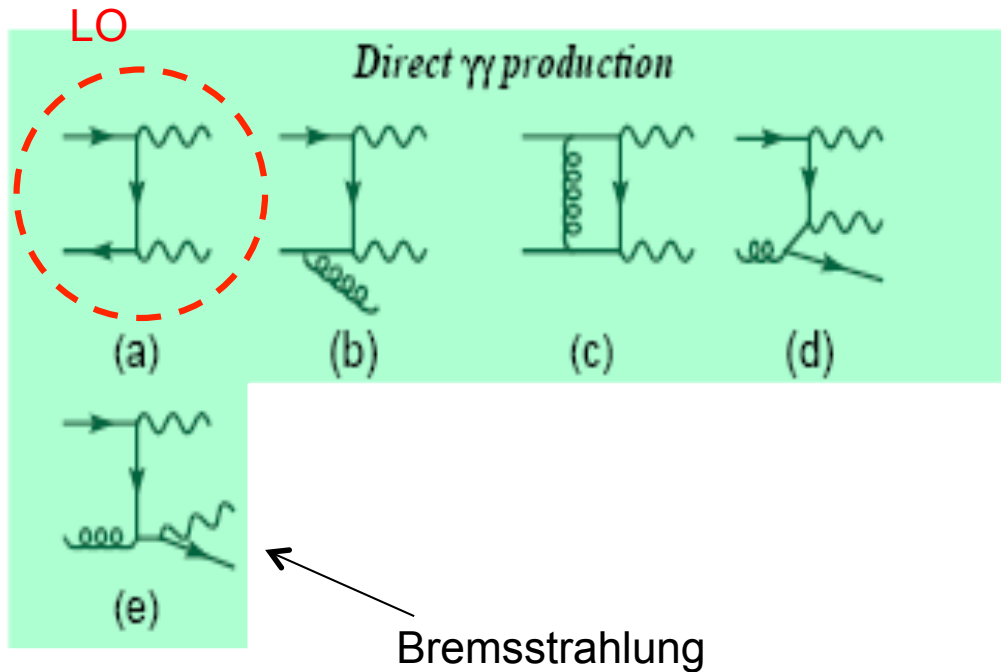
What about $H \rightarrow \gamma\gamma$ at the Tevatron?

- Very small SM production rate: ~ 3 fb at $M_H = 115$ GeV.
 - Even with 10 fb^{-1} /experiment, no observation expected at the Tevatron.
 - However, this channel contributes to SM Higgs sensitivity in the difficult intermediate mass region ~ 125 GeV.



Sensitivity could be improved
via multivariate analysis

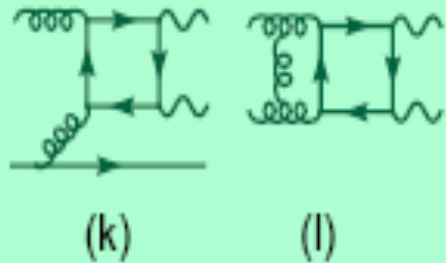
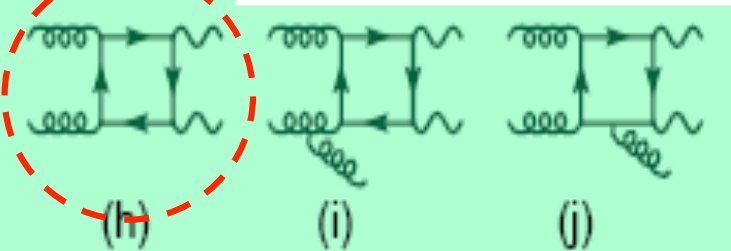
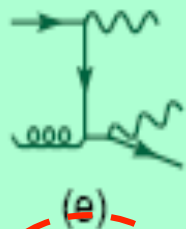
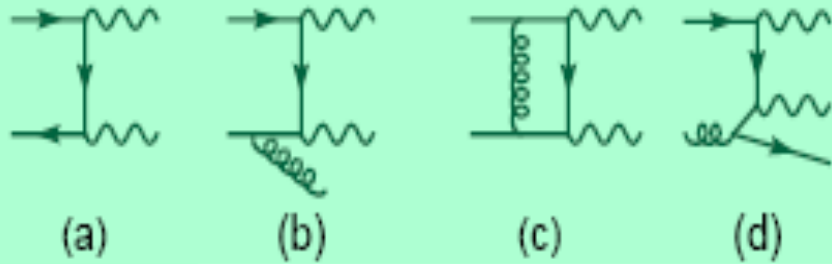
Prompt diphoton production processes



- Several classes of production processes:
 - Direct
 - Fragmentation
- **Leading order: $q\bar{q}$ scattering.**
- **Important contributions at NLO:**
 - Real emission (adds qg initiated processes)
 - Virtual corrections

Prompt diphoton production processes

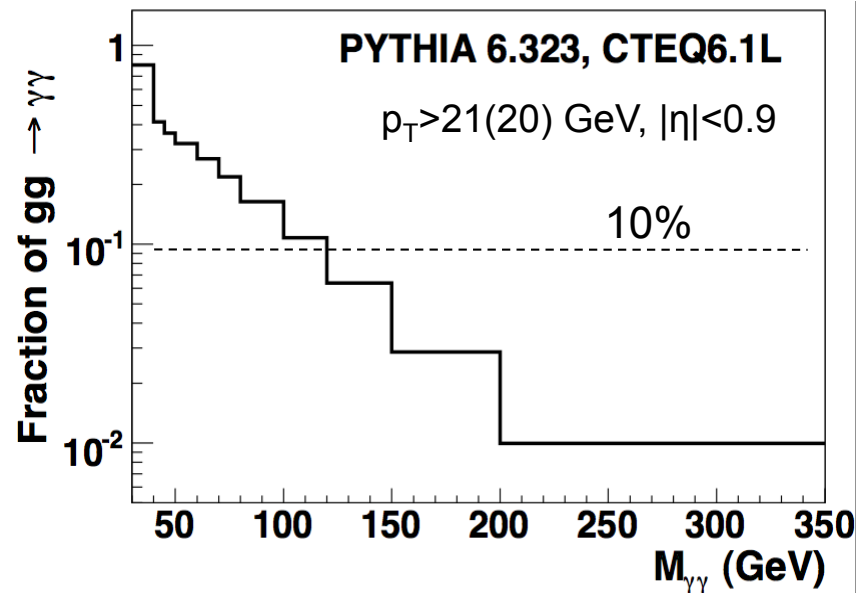
Direct $\gamma\gamma$ production



- Several classes of production processes:

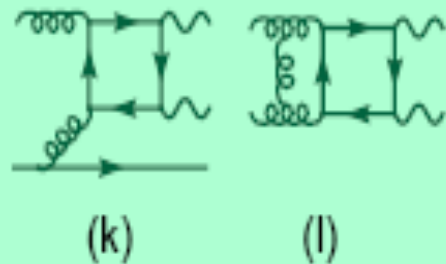
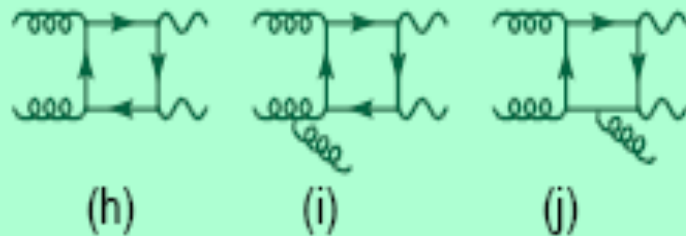
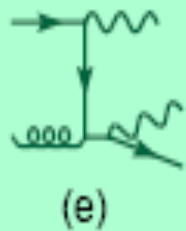
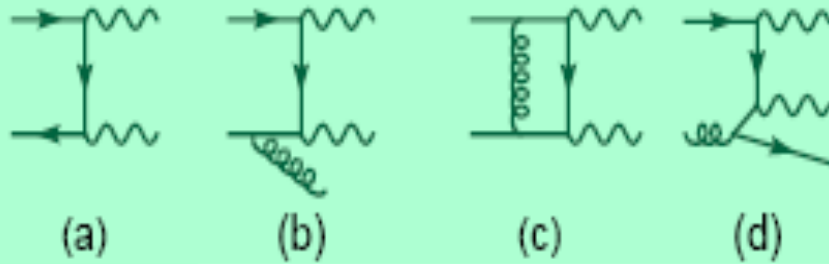
- Direct
- Fragmentation

- **gg scattering**: despite $O(\alpha_s^2)$ suppression relative to $q\bar{q} \rightarrow \gamma\gamma$, the large gluon luminosity can make this contribution sizable in particular kinematic regions.



Prompt diphoton production processes

Direct $\gamma\gamma$ production

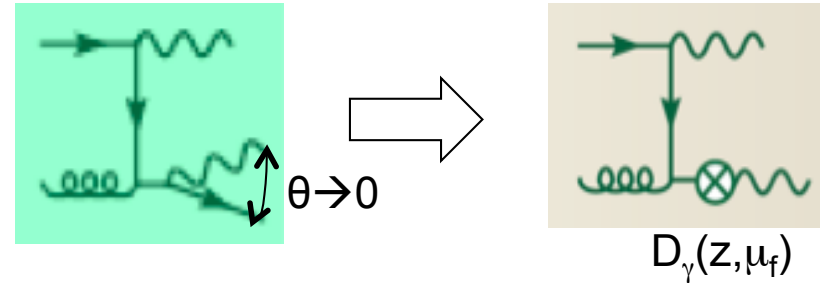


- Several classes of production processes:
 - Direct
 - Fragmentation
- Several sources of enhanced logarithmic corrections:
 - From initial state radiation
 - From final state collinear singularities
 - From possible small-x logs

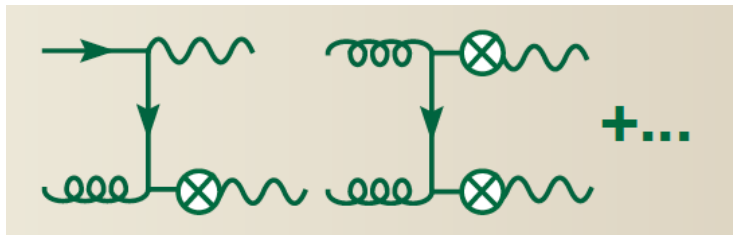
Quite an interesting process to put to the test our ability to make precise QCD predictions!

Fragmentation contributions

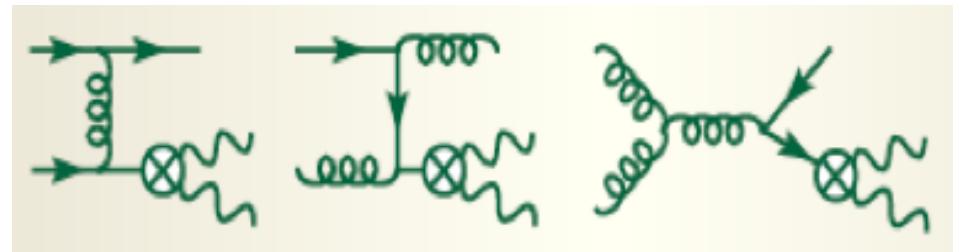
- Collinear singularity in final state photon radiation off a parton can be handled e.g. via fragmentation functions.



Single-photon fragmentation



Double-photon fragmentation



Low-mass/small-angle diphoton pairs



Not included in any theoretical prediction!

- Fragmentation contributions can be suppressed via:
 - experimental photon isolation requirements (can only be approximated in theory)
 - $p_T(\gamma\gamma) < M(\gamma\gamma)$

$$E_T^{iso} = \sum_{\text{partons or hadrons within } \Delta R < 0.4} p_{T,i} - p_{T\gamma}$$

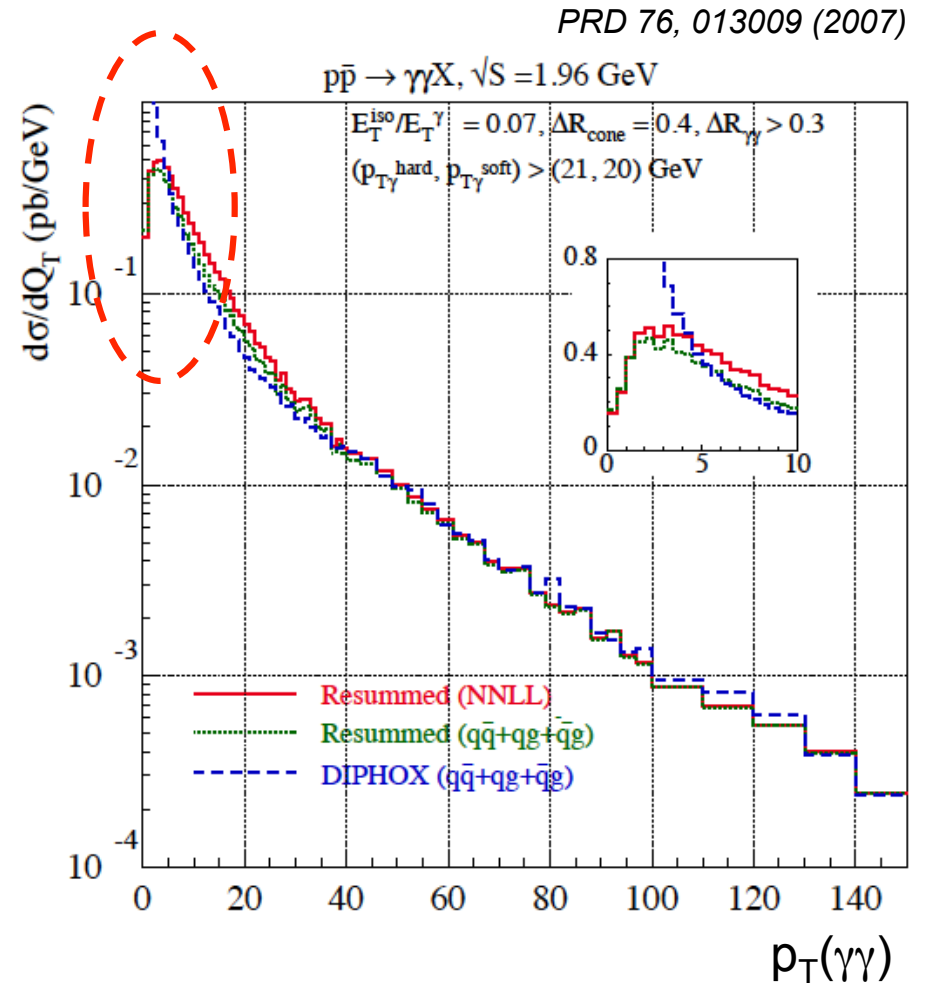
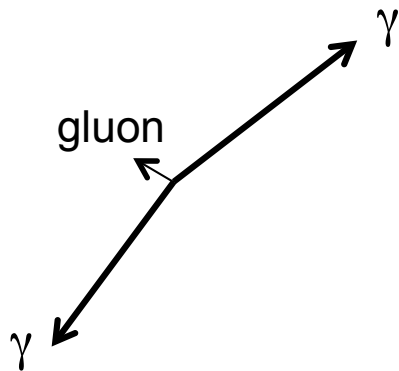
Resummation of initial state gluons

- At fixed $M(\gamma\gamma)$, the differential cross section as a function of $p_T(\gamma\gamma)$ at $O(\alpha_s)$ given by:

$$\frac{d\sigma}{dp_{T\gamma\gamma}^2} = \sigma_0 \frac{\alpha_s}{\pi} \frac{1}{p_{T\gamma\gamma}^2} \left[a \ln\left(\frac{M_{\gamma\gamma}^2}{p_{T\gamma\gamma}^2}\right) + a_0 \right]$$

Fixed-order calculation less reliable for $p_T(\gamma\gamma) \ll M(\gamma\gamma)$ and diverges as $p_T(\gamma\gamma) \rightarrow 0$.

[Also when $\Delta\phi(\gamma,\gamma) \rightarrow \pi$.]



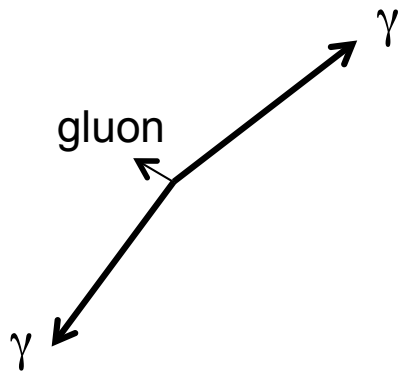
Resummation of initial state gluons

- At fixed $M(\gamma\gamma)$, the differential cross section as a function of $p_T(\gamma\gamma)$ is given by:

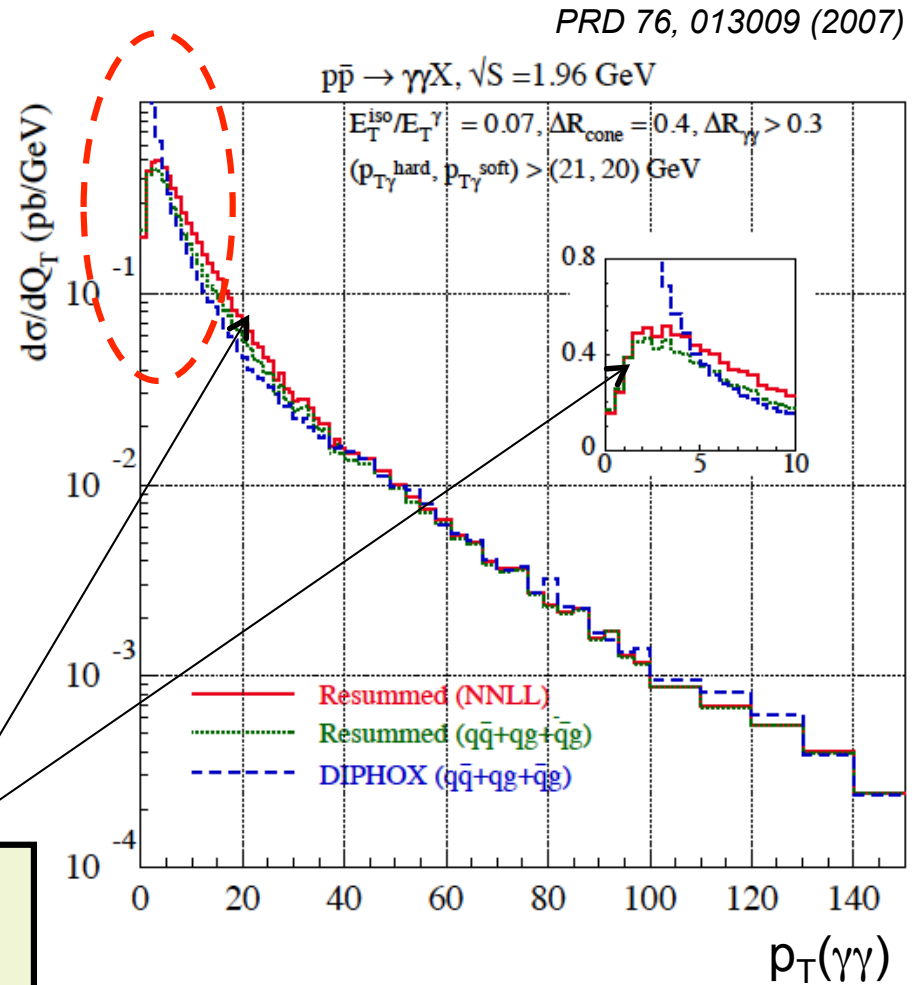
$$\frac{d\sigma}{dp_{T\gamma\gamma}^2} = \sigma_0 \frac{\alpha_s}{\pi} \frac{1}{p_{T\gamma\gamma}^2} \left[a \ln\left(\frac{M_{\gamma\gamma}^2}{p_{T\gamma\gamma}^2}\right) + a_0 \right]$$

Fixed-order calculation less reliable for $p_T(\gamma\gamma) \ll M(\gamma\gamma)$ and diverges as $p_T(\gamma\gamma) \rightarrow 0$.

[Also when $\Delta\phi(\gamma,\gamma) \rightarrow \pi$.]



Physical description of the $p_T(\gamma\gamma)$ and $\Delta\phi(\gamma,\gamma)$ distributions requires all-order resummation of soft and collinear logarithms.



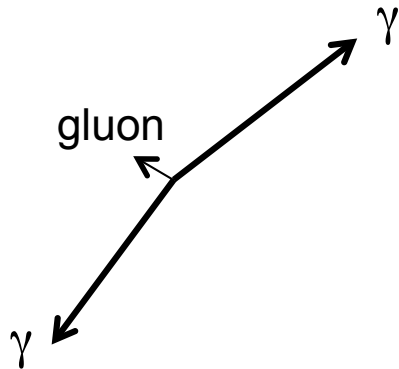
Resummation of initial state gluons

- At fixed $M(\gamma\gamma)$, the differential cross section as a function of $p_T(\gamma\gamma)$ is given by:

$$\frac{d\sigma}{dp_{T\gamma\gamma}^2} = \sigma_0 \frac{\alpha_s}{\pi} \frac{1}{p_{T\gamma\gamma}^2} \left[a \ln\left(\frac{M_{\gamma\gamma}^2}{p_{T\gamma\gamma}^2}\right) + a_0 \right]$$

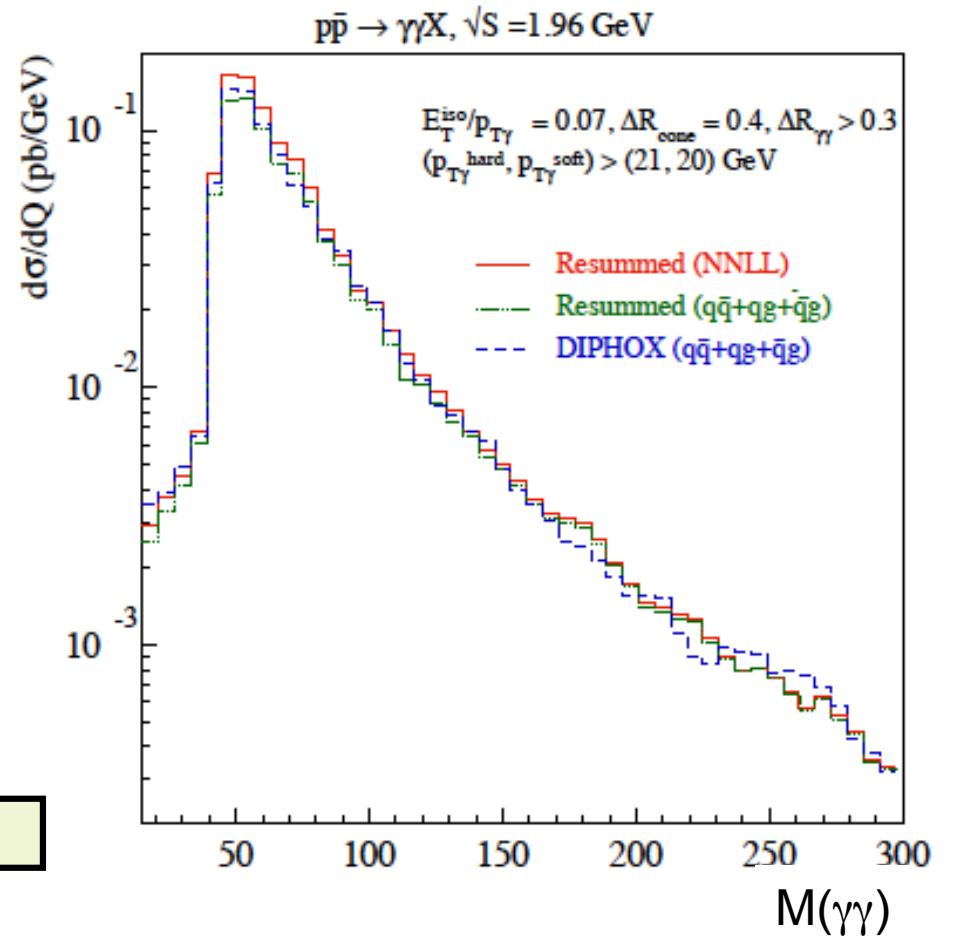
Fixed-order calculation less reliable for $p_T(\gamma\gamma) \ll M(\gamma\gamma)$ and diverges as $p_T(\gamma\gamma) \rightarrow 0$.

[Also when $\Delta\phi(\gamma,\gamma) \rightarrow \pi$.]



Only small effect on $M(\gamma\gamma)$ from resummation

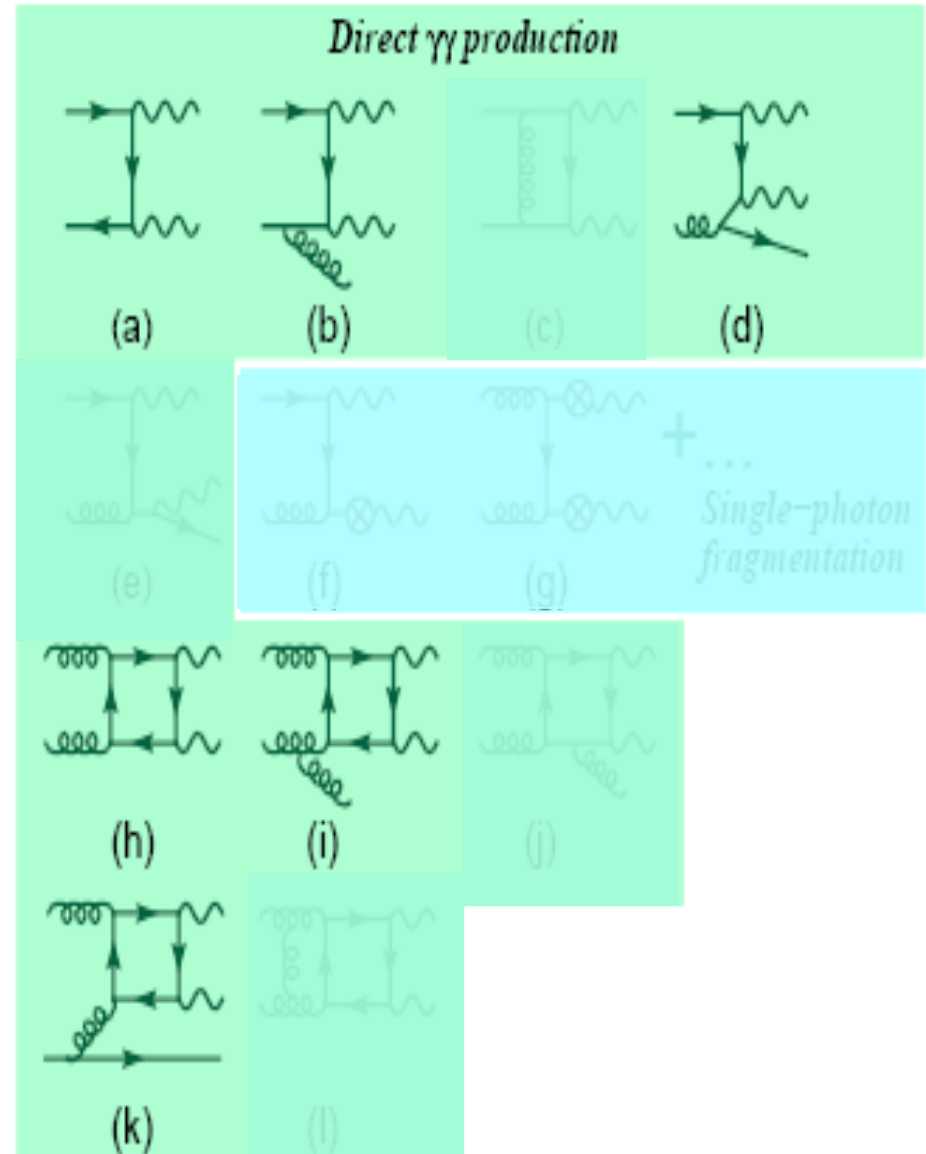
PRD 76, 013009 (2007)



Theoretical predictions

PYTHIA

- $qq \rightarrow \gamma\gamma$ and $gg \rightarrow \gamma\gamma$ matrix elements.
- All-orders resummation to LL accuracy via parton shower.
- No fragmentation contributions included.



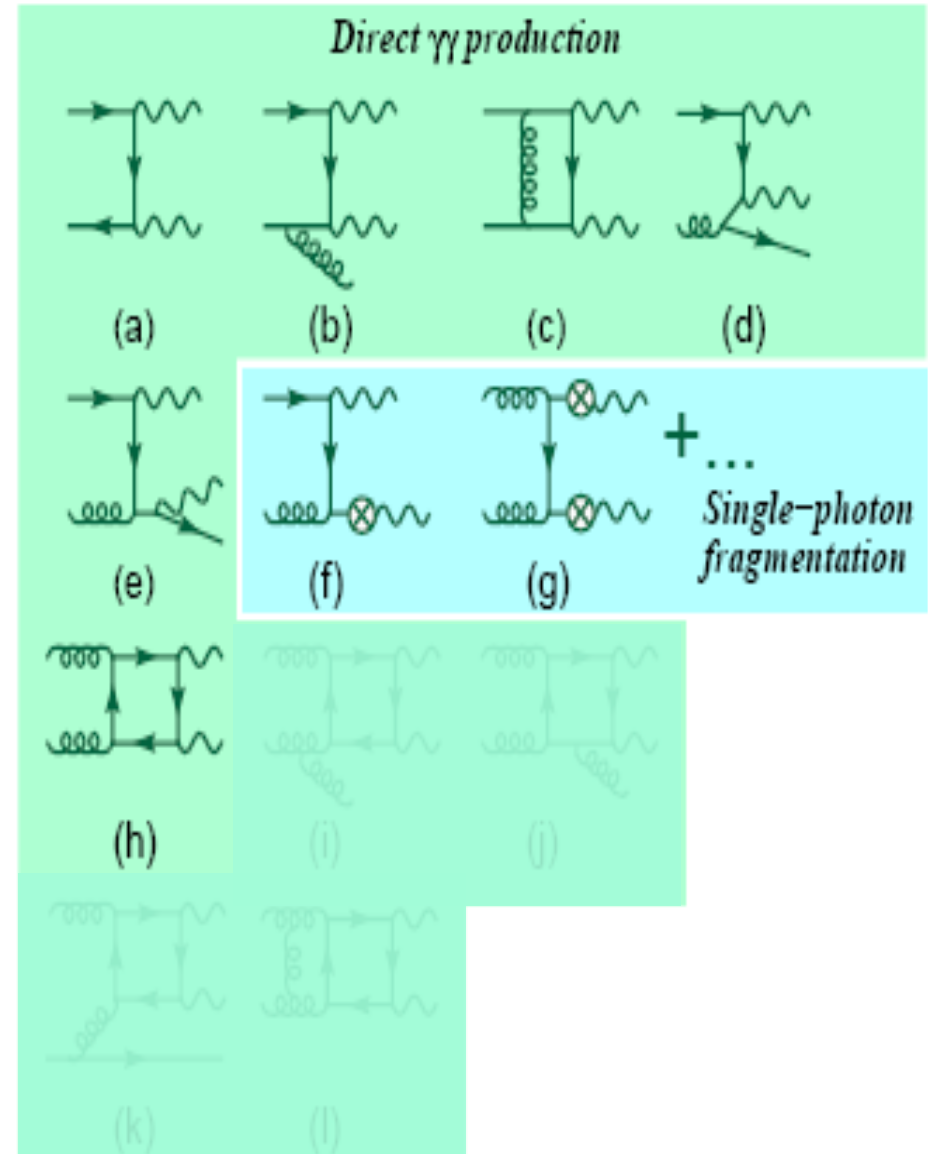
Theoretical predictions

PYTHIA

- $qq \rightarrow \gamma\gamma$ and $gg \rightarrow \gamma\gamma$ matrix elements.
- All-orders resummation to LL accuracy via parton shower.
- No fragmentation contributions included.

DIPHOX *Eur. Phys. J. C 16, 311 (2000)*

- Fixed-order NLO calculation (except for $gg \rightarrow \gamma\gamma$, which is at LO)
- No resummation:
 - ➔ usually avoid divergence by requiring asymmetric $p_{T\gamma 1} - p_{T\gamma 2} > 0$.
- Single-photon fragmentation (to NLO) included.



Theoretical predictions

PYTHIA

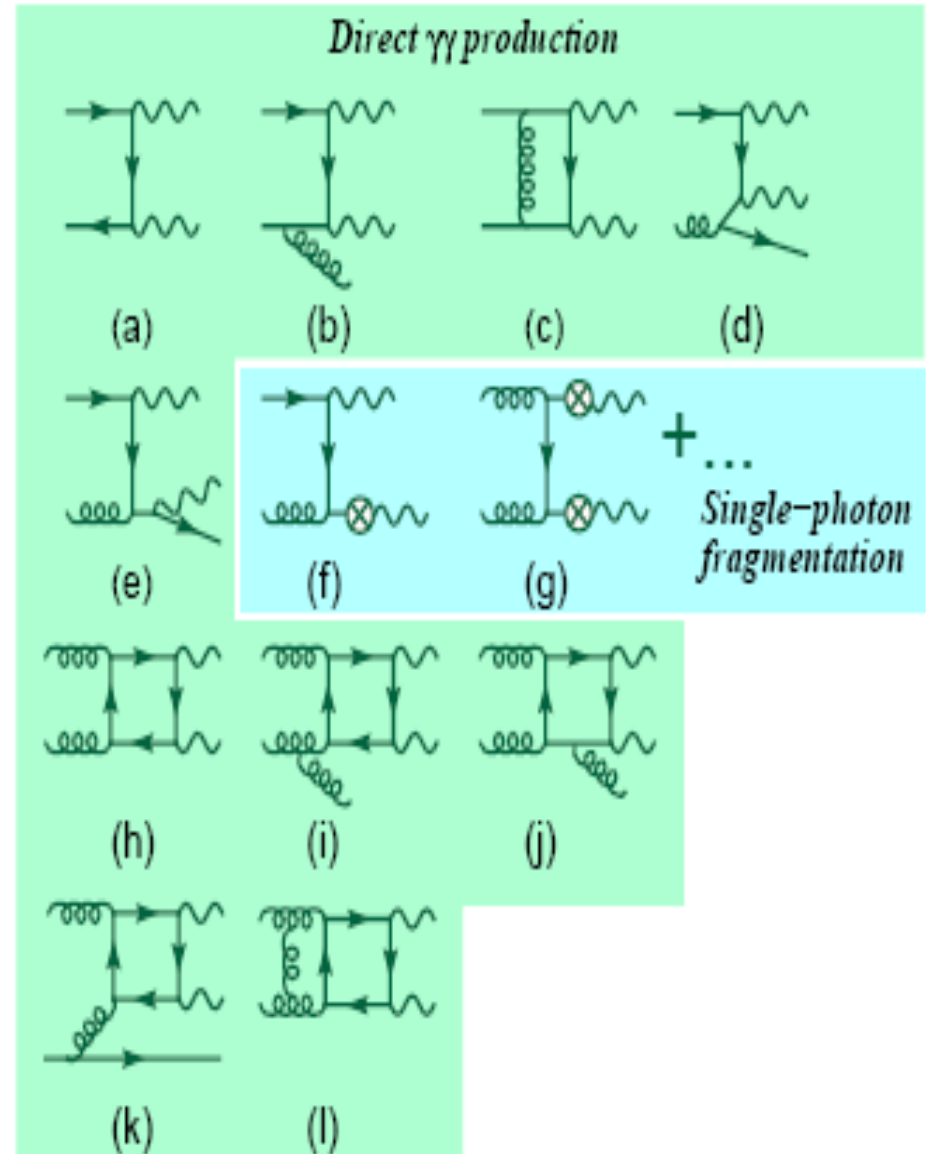
- $qq \rightarrow \gamma\gamma$ and $gg \rightarrow \gamma\gamma$ matrix elements.
- All-orders resummation to LL accuracy via parton shower.
- No fragmentation contributions included.

DIPHOX *Eur. Phys. J. C 16, 311 (2000)*

- Fixed-order NLO calculation (except for $gg \rightarrow \gamma\gamma$, which is at LO)
- No resummation:
 - usually avoid divergence by requiring asymmetric $p_{T\gamma 1} - p_{T\gamma 2} > 0$.
- Single-photon fragmentation (to NLO) included.

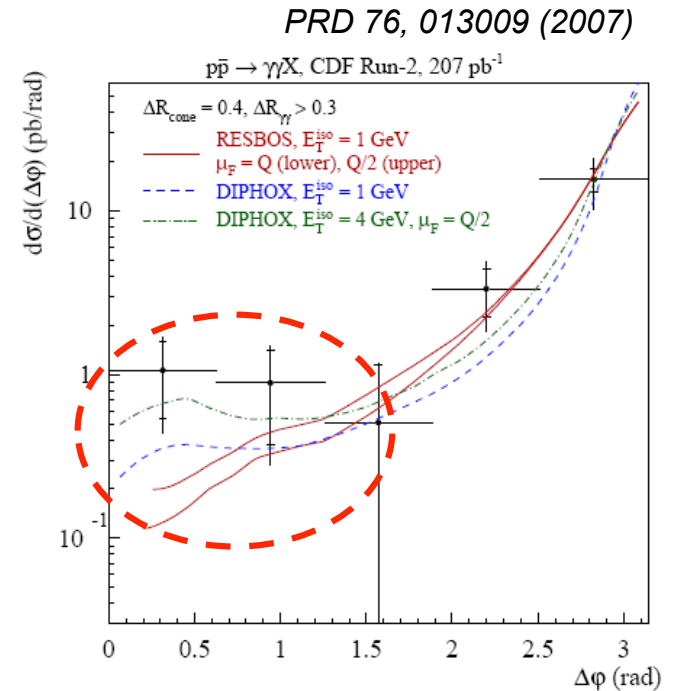
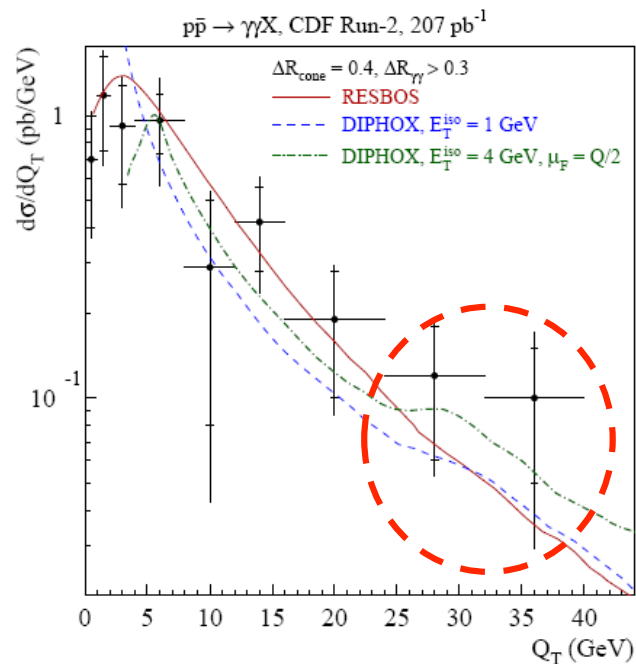
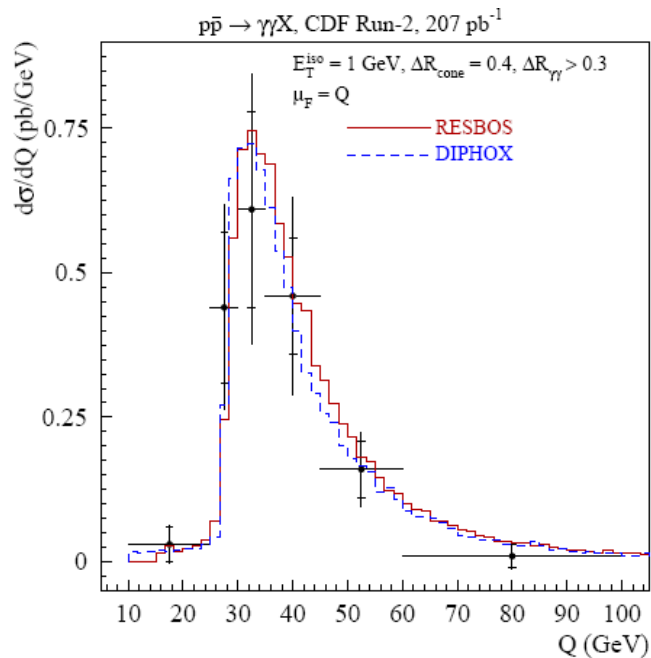
RESBOS *PRD 76, 013009 (2007)*

- All-orders resummation (to NNLL accuracy) matched to NLO.
- Single-photon fragmentation included via parameterization that approximates rate predicted by NLO fragmentation functions.



Previous Tevatron measurements

- CDF publication in Run II with 207 pb⁻¹. *PRL 95, 022003 (2005)*
- Event selection: $p_{T1(2)}=14(13)$ GeV, $|\eta_{1,2}|<0.9$, $\Delta R(\gamma,\gamma)<0.3$, $E_T^{\text{iso}}<1$ GeV.

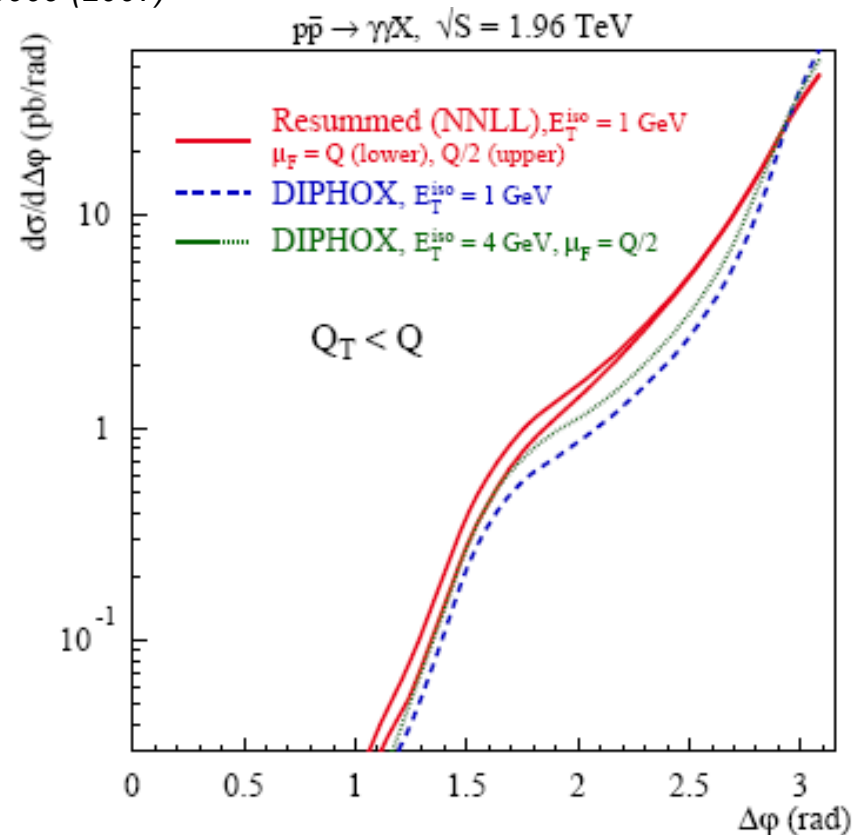
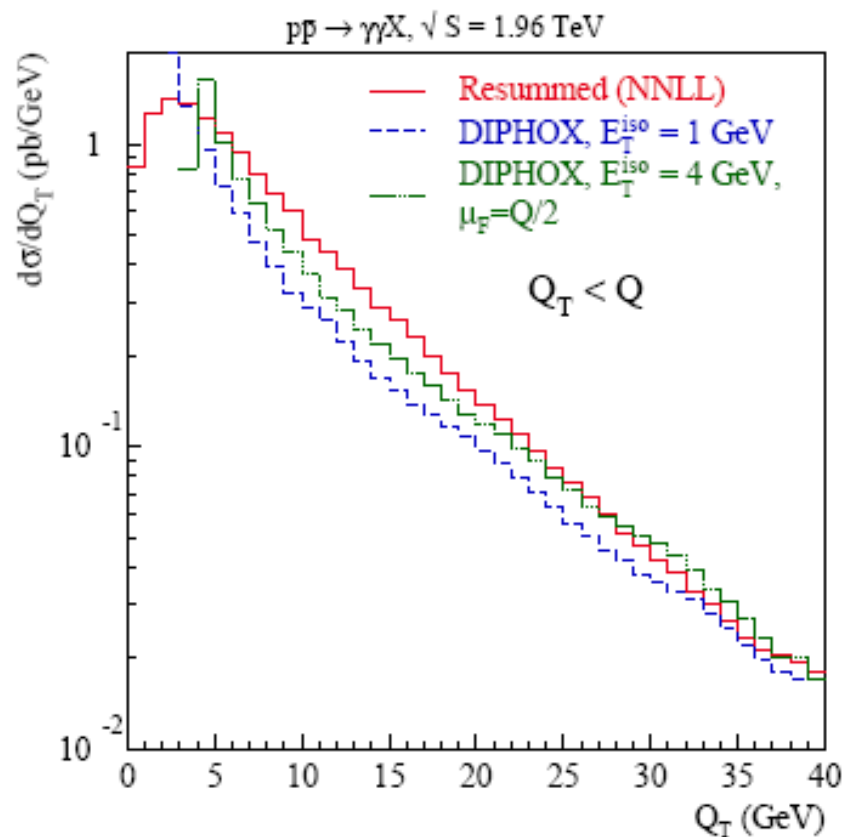


- No requirement of $p_T(\gamma\gamma)<M(\gamma\gamma)$.
- $p_T(\gamma\gamma)>25$ GeV region in data dominated by events with $p_T(\gamma\gamma)>M(\gamma\gamma)$ and $\Delta\phi(\gamma,\gamma)<\pi/2 \rightarrow$ potentially large double-fragmentation contribution.
- Large sensitivity of theoretical prediction on isolation requirement.

Getting more robust theoretical predictions

- Requirement $p_T(\gamma\gamma) < M(\gamma\gamma)$ significantly reduces contribution from fragmentation processes and thus reduce dependence of predictions on tunable isolation parameters and factorization scale.

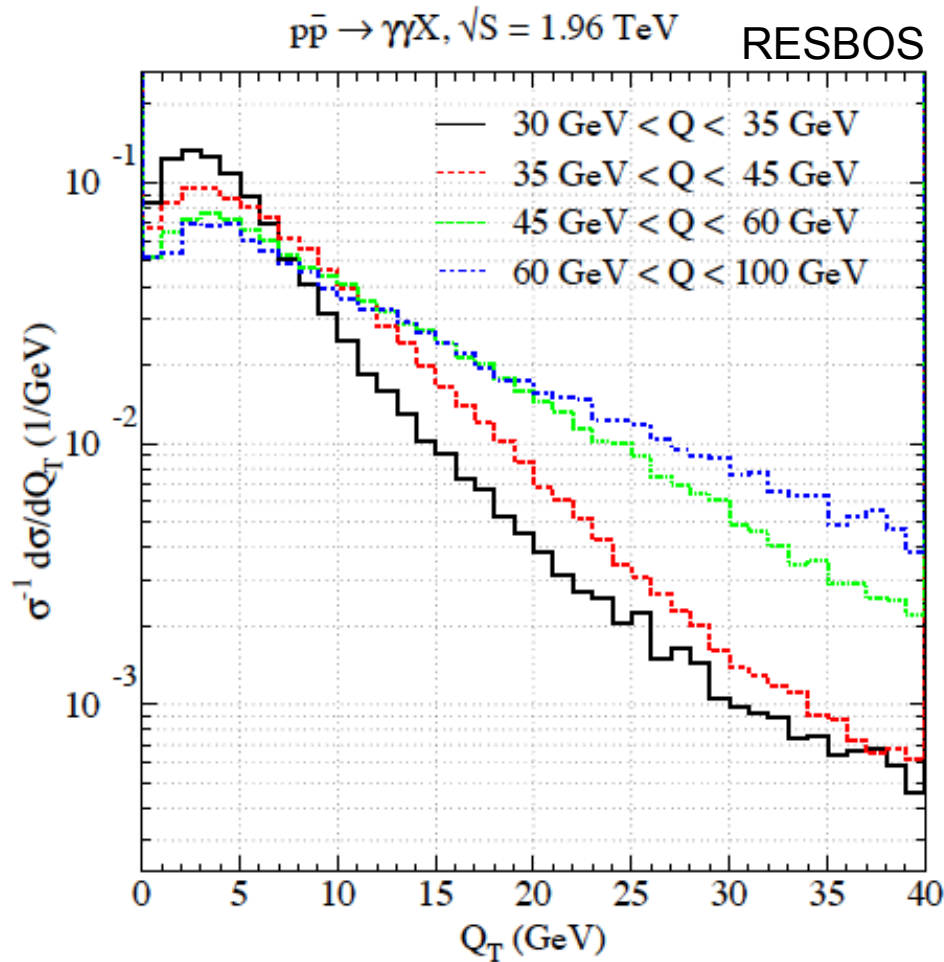
PRD 76, 013009 (2007)



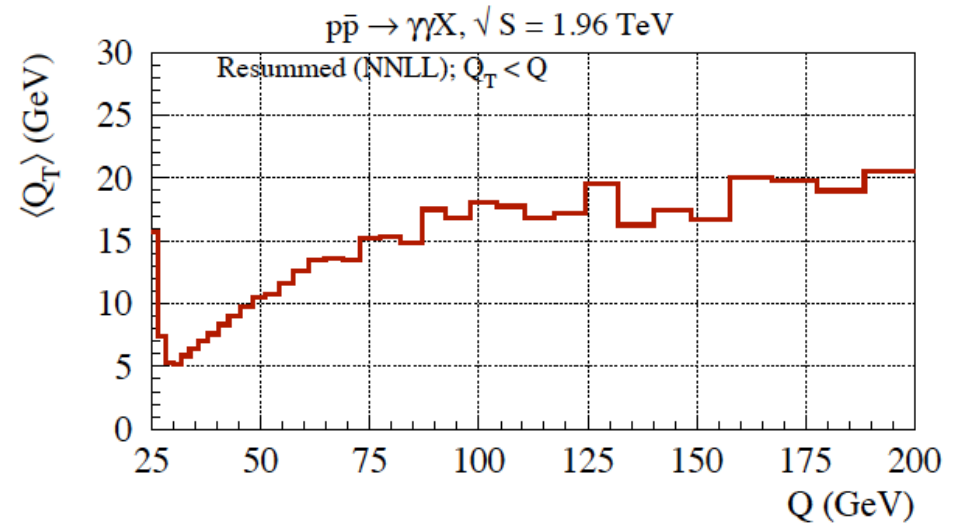
- restricts data-to-theory comparisons to region where theory is best understood and uncertainties are smaller.

Predicted double differential cross sections

- An important prediction of the resummed calculation is the broadening of the $p_T(\gamma\gamma)$ distribution with increasing $M(\gamma\gamma)$.



PRD 76, 013009 (2007)



Prediction uses same cuts as in CDF publication.

Scope of this measurement

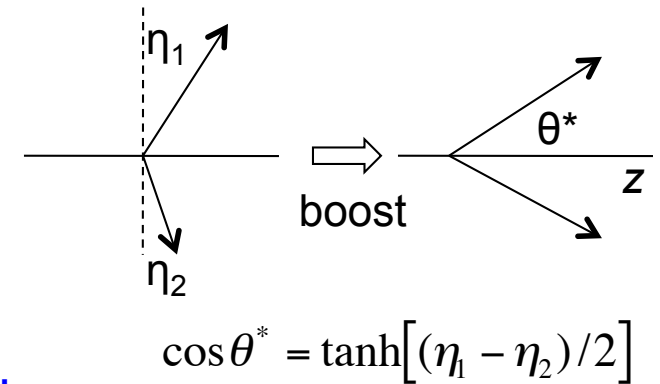
- Measurement of unfolded differential cross sections as functions of four complementary observables:

Sensitive to ISR and fragmentation

Sensitive to PDFs

$$\frac{d\sigma}{dM_{\gamma\gamma}} \quad \frac{d\sigma}{dp_T^{\gamma\gamma}} \quad \frac{d\sigma}{d\Delta\phi_{\gamma\gamma}} \quad \frac{d\sigma}{d|\cos\theta^*|}$$

Sensitive to energy scale of the interaction and to New Physics!



Also measure double-differential cross sections:

$$\frac{d^2\sigma}{dM_{\gamma\gamma} dp_T^{\gamma\gamma}} \quad \frac{d^2\sigma}{dM_{\gamma\gamma} d\Delta\phi_{\gamma\gamma}} \quad \frac{d^2\sigma}{dM_{\gamma\gamma} d|\cos\theta^*|}$$

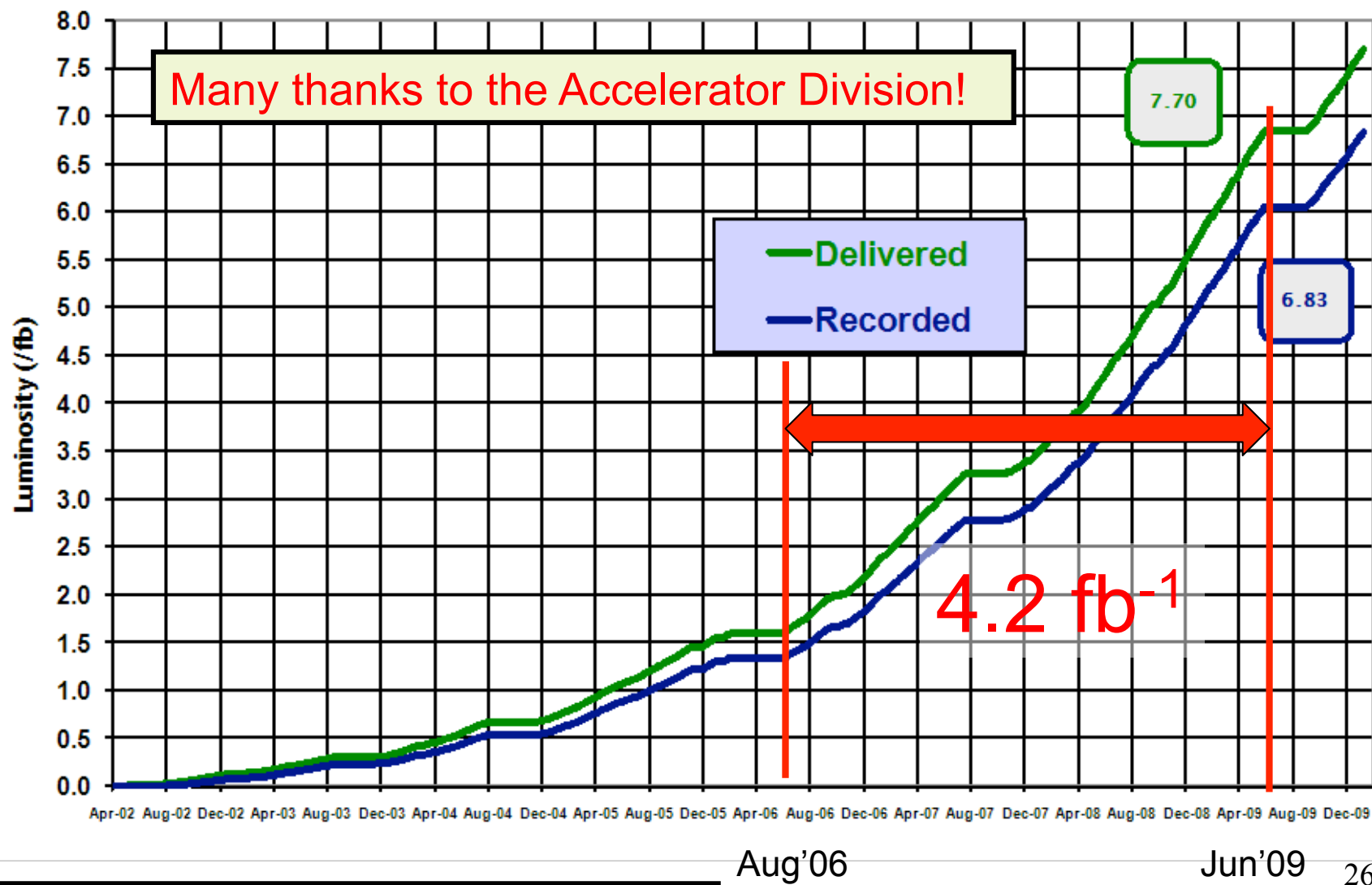
$$\left\{ \begin{array}{l} 30 \leq M_{\gamma\gamma} < 50 \text{ GeV} \\ 50 \leq M_{\gamma\gamma} < 80 \text{ GeV} \\ 80 \leq M_{\gamma\gamma} < 350 \text{ GeV} \end{array} \right.$$

Data set



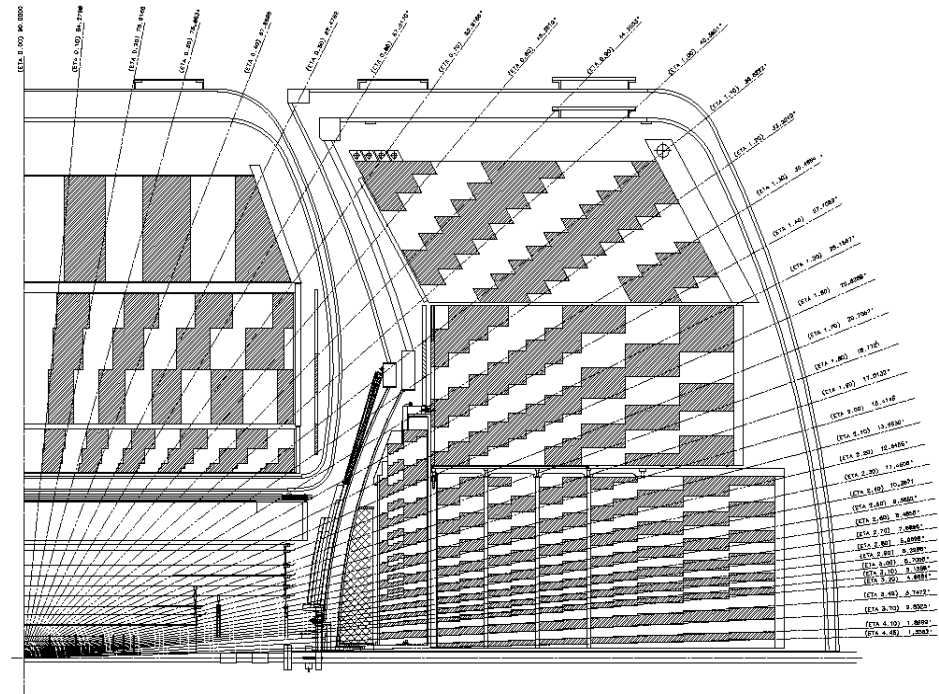
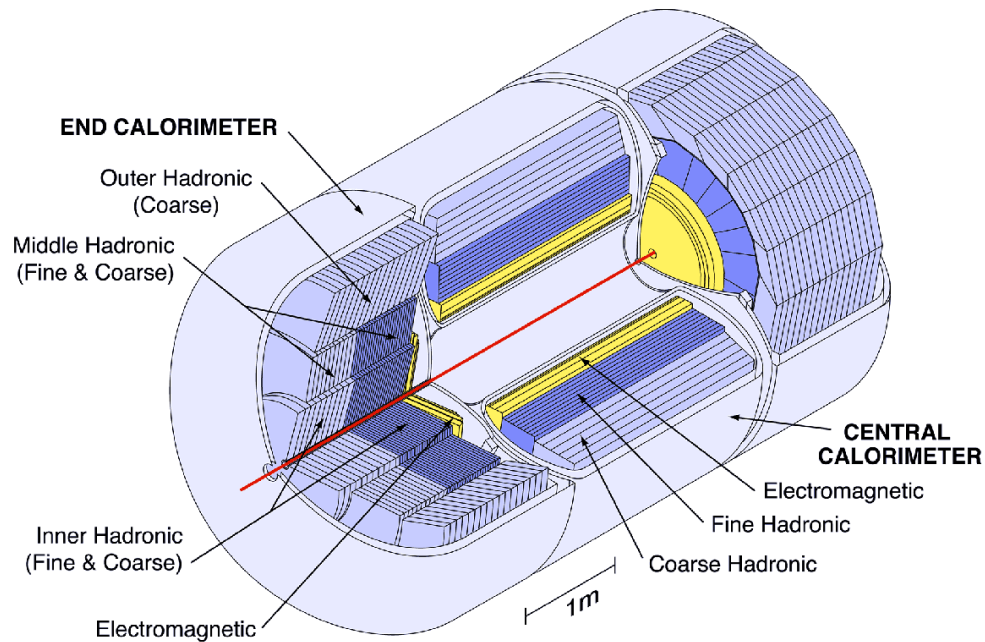
Run II Integrated Luminosity

19 April 2002 - 24 January 2010



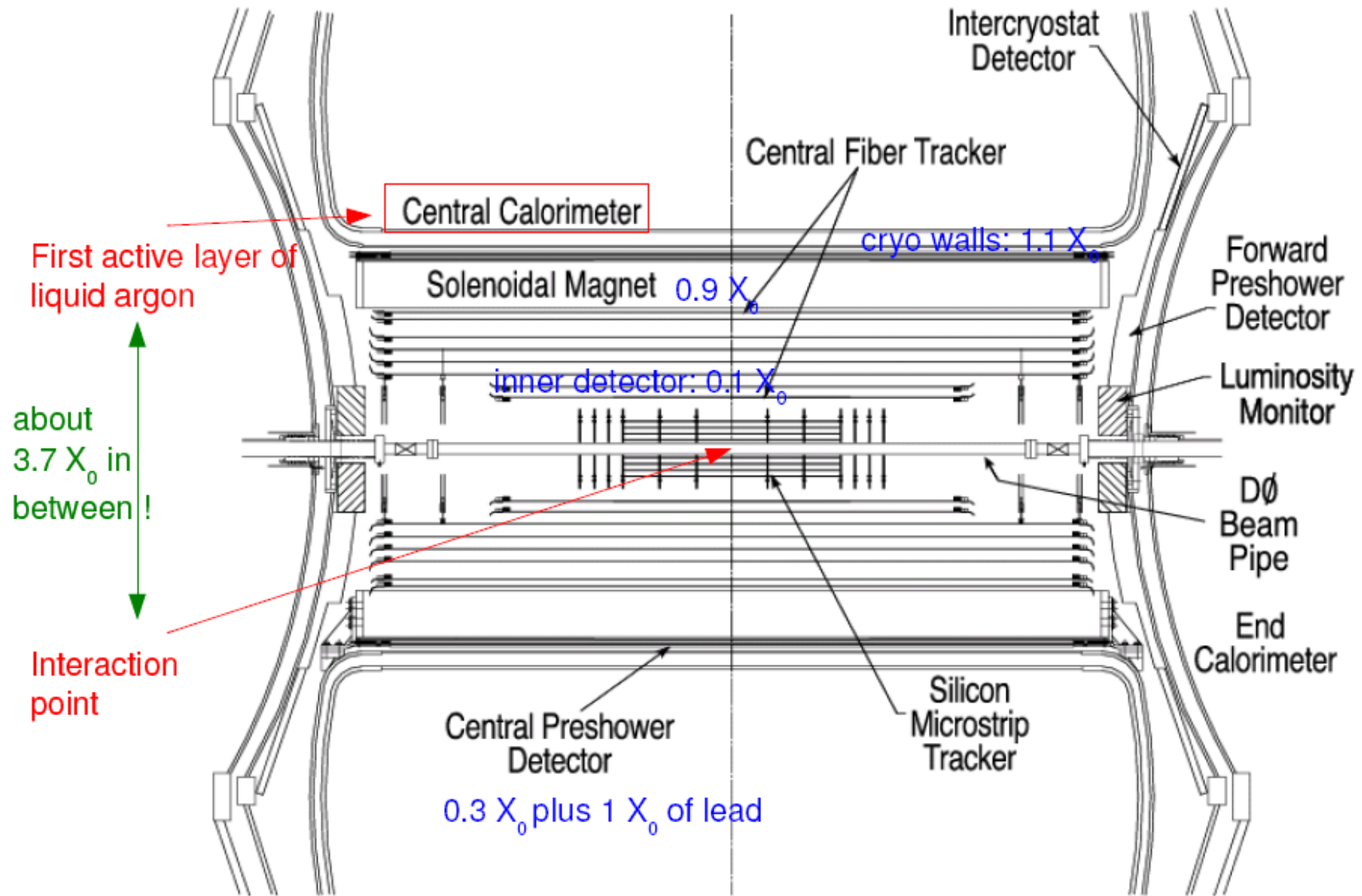
x20 more luminosity than previous publication!

Calorimeter overview



- Liquid argon active medium and (mostly) uranium absorber.
- Electromagnetic calorimeter:
 - 4 layers, $\sim 20 X_0$.
 - Coverage: $|\eta| < 1.1$ and $1.5 < |\eta| < 3.2$.
 - Segmentation (towers): $\Delta\eta \times \Delta\phi = 0.1 \times 0.1$ (except in 3rd EM layer: 0.05×0.05).
- A significant change in Run II:
 - Added solenoid and preshower detector before calorimeter.

Calorimeter overview



Photon identification: basic selection

- Central photons are selected from EM clusters reconstructed within a cone with radius $R=0.2$ requiring:

- High EM fraction: $>97\%$

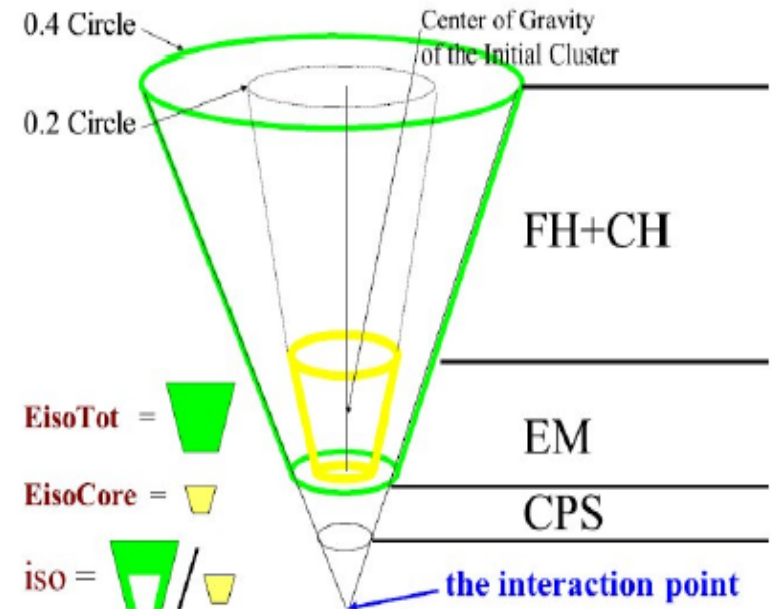
- Isolated in the calorimeter:

$$I = \frac{E_{tot}(R=0.4) - E_{EM}(R=0.2)}{E_{EM}(R=0.2)} < 0.07$$

- Isolated in the tracker:

$$p_{T,trk}^{sum} = \sum_{0.05 < R < 0.4} p_{T,trk} < 1.5 \text{ GeV}$$

- Shower width in 3rd EM layer consistent with an EM object.

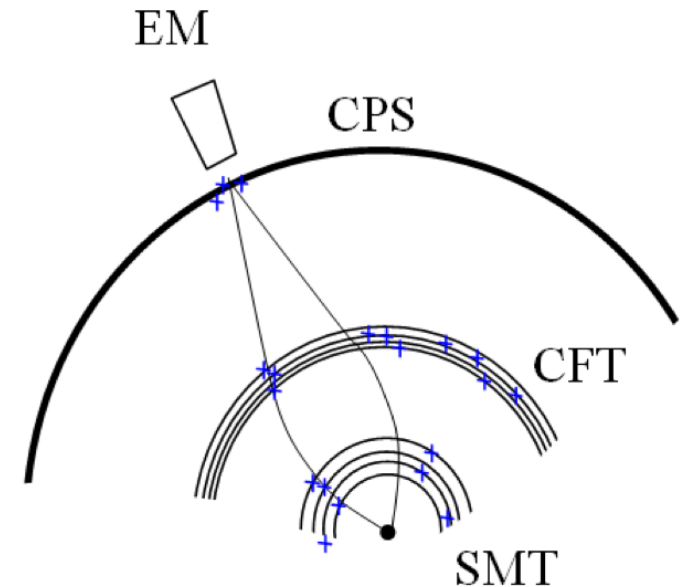
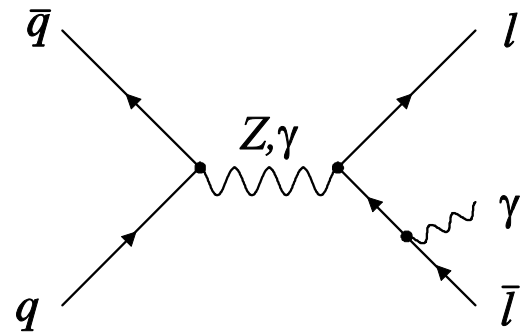


- Photon efficiency: $\sim 90-95\%$ (measured in $Z \rightarrow ee$ events).
- Agreement with MC better than 1%
 \rightarrow assigned as systematic uncertainty.

Photon identification: track veto

Track veto:

- No spatially well-matched track and
- No pattern of hits in the tracker in a road around the EM cluster consistent with an e^\pm .
- Differences between data and simulation calibrated using photons from radiative Z decays ($Z \rightarrow l^+ l^- \gamma$) and $Z \rightarrow ee$.



- **Photon efficiency: $(90 \pm 2)\%$**
- Electron misID probability: $\sim 1-4\%$ (function of ϕ).
Relative systematic uncertainty: $\sim 15\%$.

Photon identification: Neural Network

- Further improve photon purity by constructing a NN discriminant using five well-modeled variables:

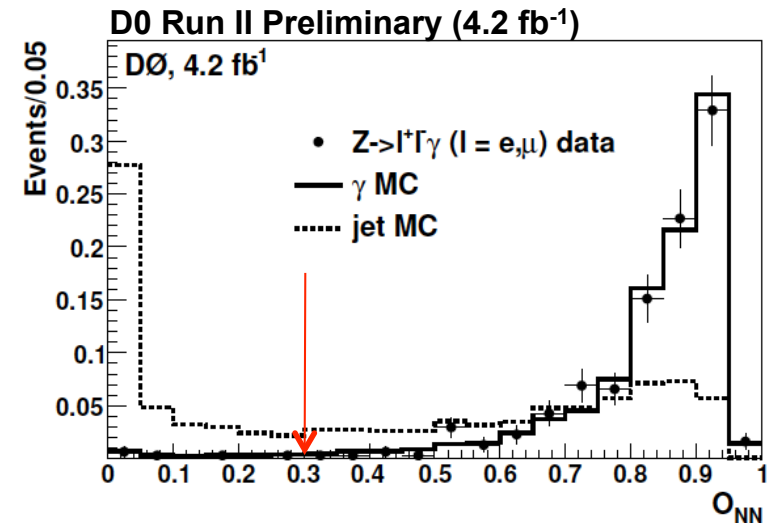
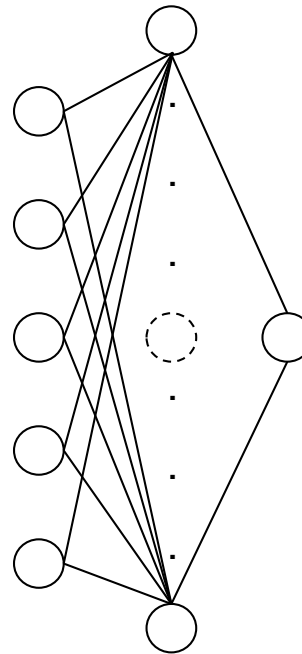
Tracker isolation ($p_{T, \text{sum, trk}}$)

Number of EM1 cells within $R < 0.2$

Number of EM1 cells within $0.2 < R < 0.4$

Number CPS clusters within $R < 0.1$

Squared-energy-weighted width of energy deposition in the CPS



- Trained using QCD $\gamma\gamma$ and dijet MC (including particle-level selections to increase the fraction of electromagnetic jets). Excellent agreement between data and MC.
- Require $NN > 0.3$:

- Photon efficiency: 98%. Systematic uncertainty: 1.5%.
- Rejects ~40% of misidentified jets.

Photon energy scale and resolution

The presence of dead material leads to:

- significant dependence of EM response and resolution on incident angle.
- different energy-loss corrections between electrons and photons.

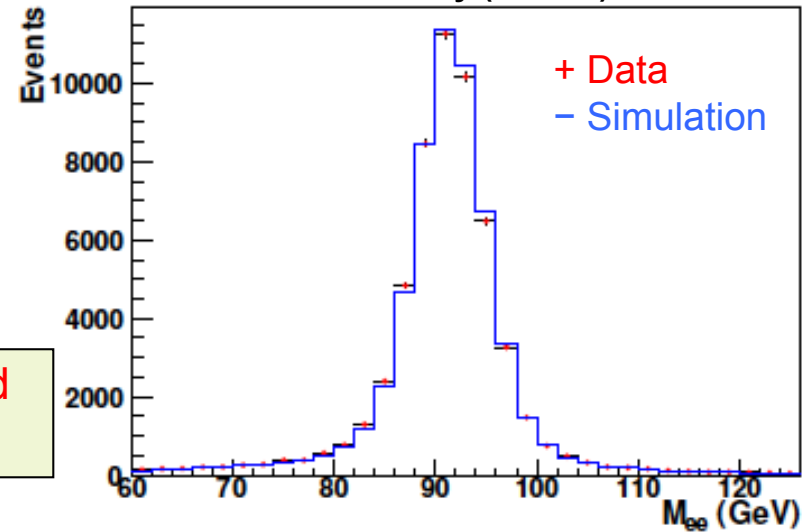
Capitalize on the detailed understanding achieved and tools developed for the M_W measurement at D0

→ Use parameterized simulation of electron response and resolution used in the M_W measurement, supplemented with dedicated photon energy scale corrections derived using tuned GEANT simulation.

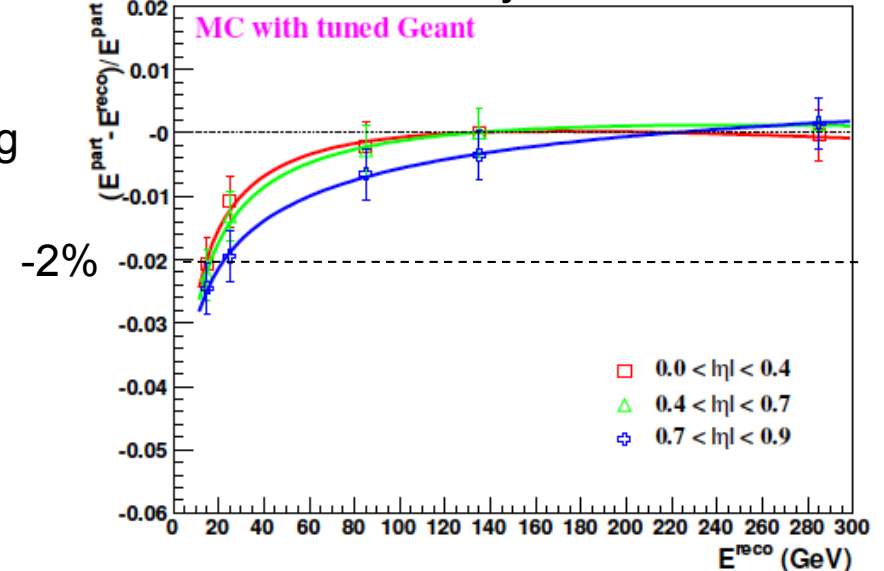
Systematic uncertainties:

- Energy scale: $\pm 0.5\%$
- Energy resolution: $\pm 5\%$ in constant term

D0 Run II Preliminary (4.2 fb⁻¹)



D0 Run II Preliminary



Event selection

- Data collected using suite of calorimeter-only di-EM triggers (p_T thresholds vary within 15-25 GeV).

→ Trigger efficiency after offline selection ~100%.

- Event selection:

Avoids divergence in NLO calculation

- 2 photons with $p_T > 21(20)$ GeV,
 $|\eta_{\text{det}}| < 0.9$, $|\eta| < 0.9$, away from CAL module boundaries in ϕ

- $\Delta R(\gamma, \gamma) > 0.4$
 - $p_T(\gamma\gamma) < M(\gamma\gamma)$
- } Helps suppress contribution from fragmentation diagrams (<6.5%)

- Primary vertex with highest number of tracks required to have $|z_{PV}| < 60$ cm. Photon kinematics computed with respect to this vertex.

→ primary vertex selection efficiency: ~98%

→ probability to match the correct primary vertex: ~65% (measured in $Z \rightarrow ee$ data)

Assign a conservative 23% relative systematic uncertainty.

Misvertexing effect implemented in parameterized simulation.

Differential cross section calculation

$$\frac{d\sigma}{dX} = \frac{N_{\gamma\gamma}}{\varepsilon \cdot A \cdot L \cdot \Delta}; \quad X = M_{\gamma\gamma}, p_T^{\gamma\gamma}, \Delta\phi_{\gamma\gamma}, |\cos\theta^*|$$

Estimated number of prompt diphoton events (points to $N_{\gamma\gamma}$)
 Event selection efficiency (points to ε)
 Event acceptance (points to A)
 Integrated luminosity (points to L)
 Bin width (points to Δ)

Measurement corresponding to the following selections at the “generator level”:

- 2 photons with $p_T > 21(20)$ GeV, $|\eta| < 0.9$, $E_T^{iso} < 2.5$ GeV
- $\Delta R(\gamma, \gamma) > 0.4$
- $p_T(\gamma\gamma) < M(\gamma\gamma)$

$$E_T^{iso} = \sum_{\substack{\text{partons or hadrons} \\ \text{within } \Delta R < 0.4}} p_{T,i} - p_{T\gamma}$$

Event acceptance

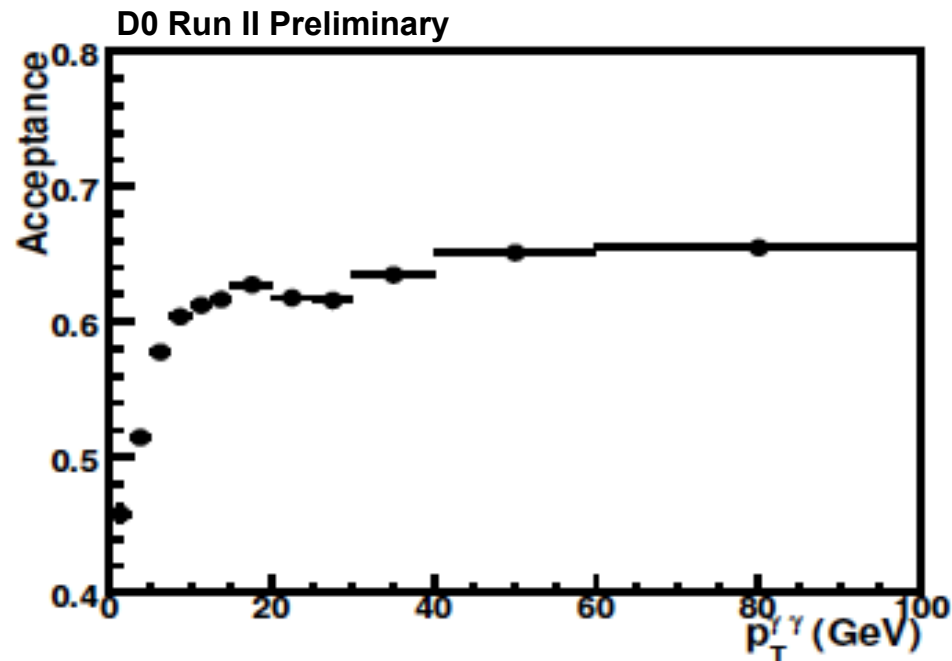
$$\frac{d\sigma}{dX} = \frac{N_{\gamma\gamma}}{\varepsilon \cdot A \cdot L \cdot \Delta}$$

- Defined as:

Number of events with two reconstructed EM clusters passing all but photon ID cuts

Number of events with two generator-level photons passing kinematic and isolation cuts

- Estimated using RESBOS (reweighted to match data) processed through the parameterized simulation including all relevant experimental effects (misvertexing, reconstruction efficiency, response, resolution, etc).



Dominant contributions:

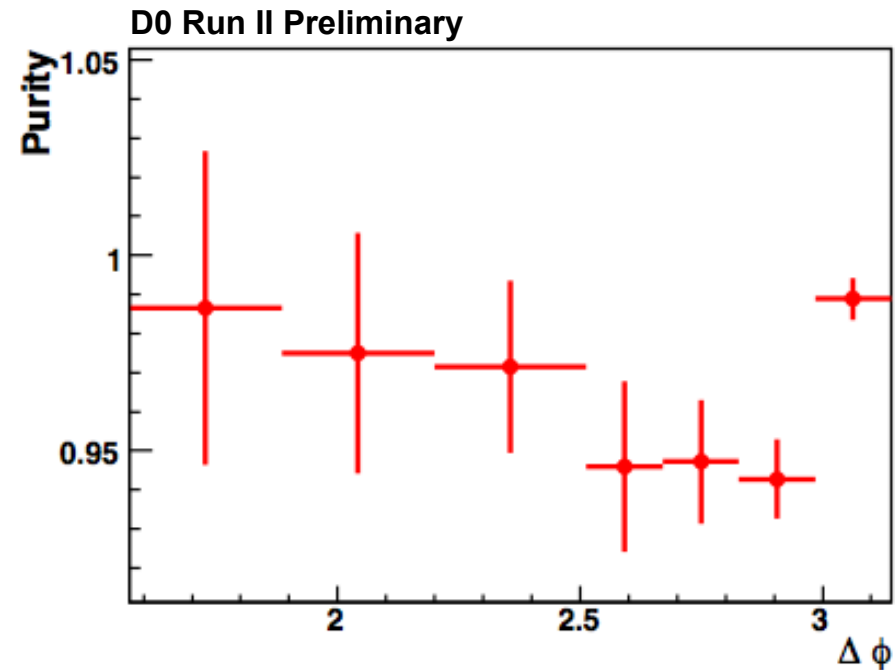
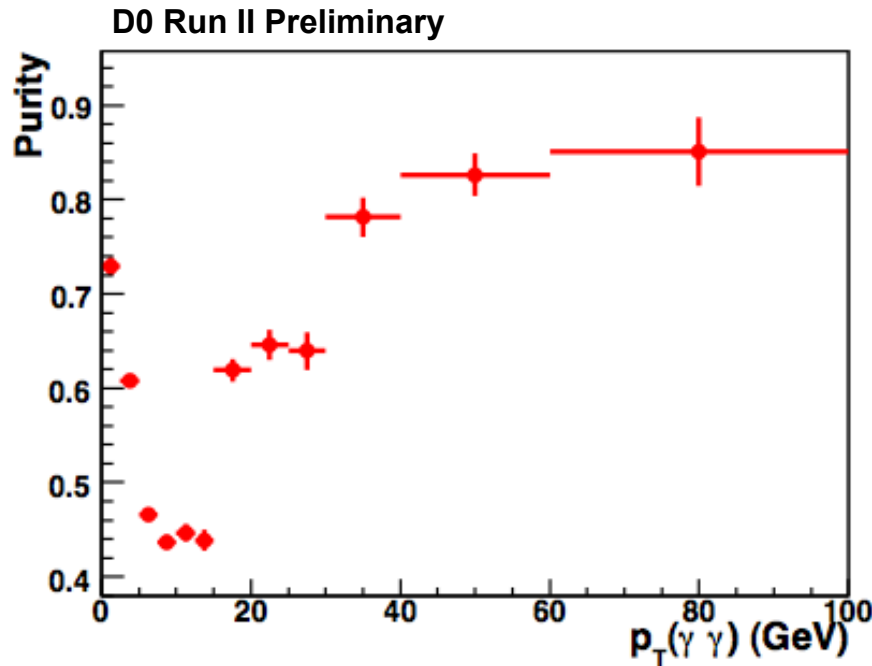
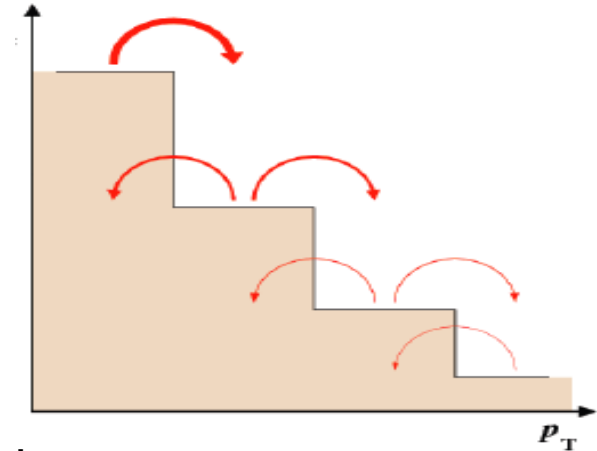
- Fiducial in ϕ
- $|\eta_{\text{det}}| < 0.9$
- Photon energy resolution
- Misvertexing

Systematic uncertainty: $\sim(3-8)\%$

Event acceptance: bin-to-bin migration

- Experimental effects (photon energy resolution, misvertexing) lead to event migration outside a given bin at the reconstructed or generated level. The magnitude of the effect depends on the bin size relative to the smearing.

$$\text{Purity (bin } i) = N(\text{gen bin } i \text{ AND reco bin } i) / N(\text{reco bin } i)$$

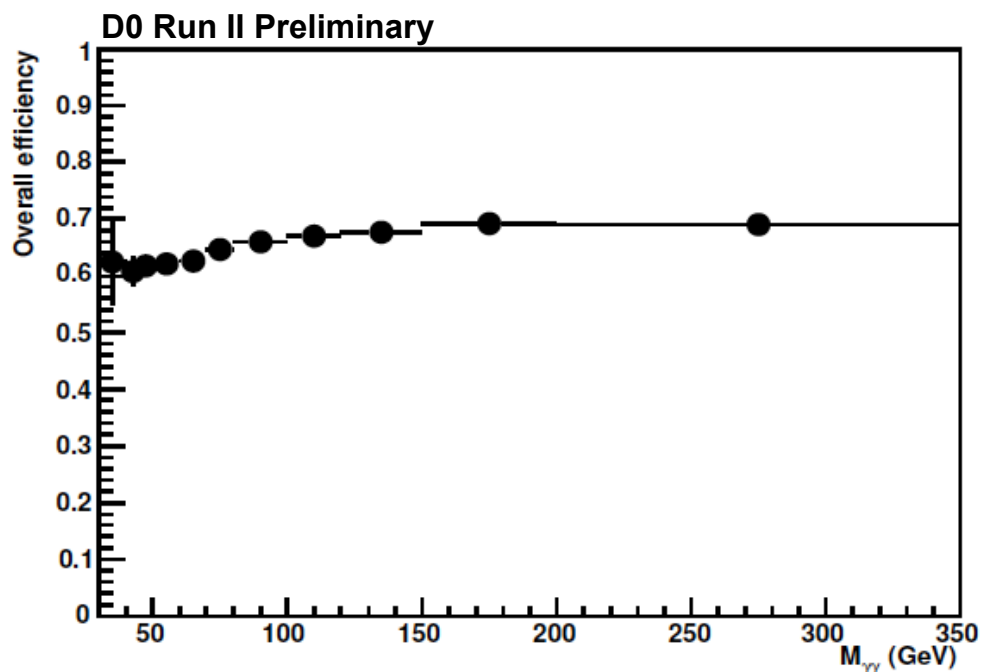


→ The acceptance correction also accounts for this.

Event selection efficiency

$$\frac{d\sigma}{dX} = \frac{N_{\gamma\gamma}}{\varepsilon \cdot A \cdot L \cdot \Delta}$$

- Includes only the efficiency of the photon selection criteria.
Overall per-photon selection efficiency: ~80%.
- Estimated using full GEANT simulation and including small corrections to match individual efficiencies measured in data.



Systematic uncertainty: 4.1%

Per-photon uncertainties:

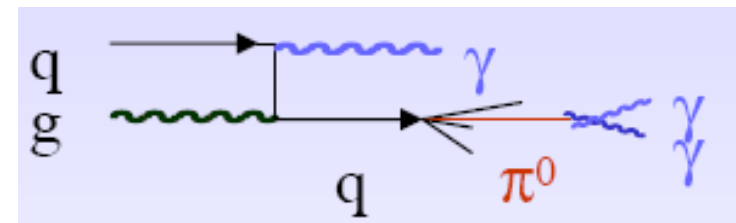
Source	Uncertainty
Basic selection	$\pm 1\%$
Track veto	$\pm 2\%$
NN selection	$\pm 1.5\%$
e/ γ difference	$\pm 1\%$
Total	$\pm 2.9\%$

Backgrounds

$$\frac{d\sigma}{dX} = \frac{N_{\gamma\gamma}}{\varepsilon \cdot A \cdot L \cdot \Delta}$$

- Electrons misidentified as photons: $Z/\gamma^* \rightarrow e^+e^-$**
 - due to inefficiency of track veto requirement.
 - estimated using MC normalized to NNLO theoretical cross section and suitable data/MC scale factors to correct selection efficiencies.
- Jets misidentified as photons: dijet and γ +jet**
 - fluctuations in jet fragmentation to leading π^0 or η^0 meson ($\pi^0, \eta^0 \rightarrow \gamma\gamma$)
 - normalization and shape estimated directly from data using photon NN information.

Data	10938	
$\gamma\gamma$	7307 ± 312 (stat)	
γ +jet	1791 ± 411 (stat)	~16%
dijet	1679 ± 281 (stat)	~15%
$Z/\gamma^* \rightarrow e^+e^-$	161 ± 10 (stat)	~1.5%



Background estimation: 4x4 Matrix Method

- Exploit different efficiency of a tighter cut ($NN > 0.6$), relative to $NN > 0.3$, for photon and jet to compute a per-event weight under the different hypotheses ($\gamma\gamma$, γ +jet and dijet):

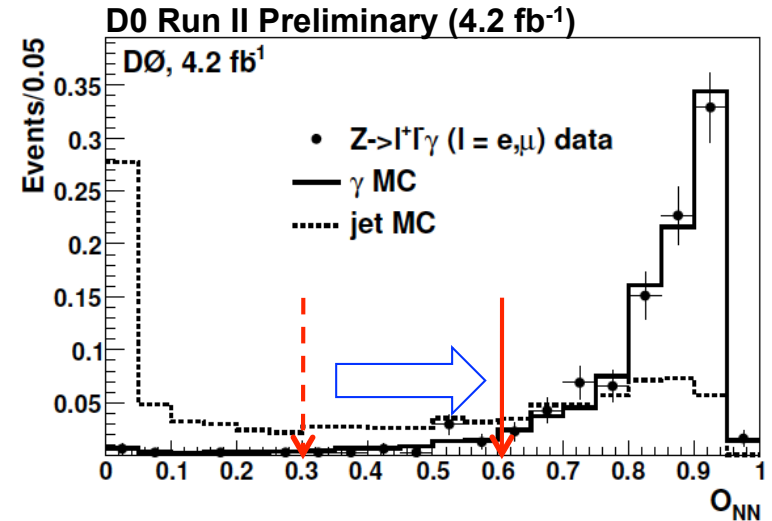
$$\begin{pmatrix} w_{jj} \\ w_{j\gamma} \\ w_{\gamma j} \\ w_{\gamma\gamma} \end{pmatrix} = E^{-1} \times \begin{pmatrix} w_{ff} \\ w_{fp} \\ w_{pf} \\ w_{pp} \end{pmatrix}$$

Both photons fail
 Leading fail, trailing passes
 Leading passes, trailing fails
 Both photons pass

$$E = \begin{pmatrix} (1 - \epsilon_{j1})(1 - \epsilon_{j2}) & (1 - \epsilon_{j1})(1 - \epsilon_{\gamma 2}) & (1 - \epsilon_{\gamma 1})(1 - \epsilon_{j2}) & (1 - \epsilon_{\gamma 1})(1 - \epsilon_{\gamma 2}) \\ (1 - \epsilon_{j1})\epsilon_{j2} & (1 - \epsilon_{j1})\epsilon_{\gamma 2} & (1 - \epsilon_{\gamma 1})\epsilon_{j2} & (1 - \epsilon_{\gamma 1})\epsilon_{\gamma 2} \\ \epsilon_{j1}(1 - \epsilon_{j2}) & \epsilon_{j1}(1 - \epsilon_{\gamma 2}) & \epsilon_{\gamma 1}(1 - \epsilon_{j2}) & \epsilon_{\gamma 1}(1 - \epsilon_{\gamma 2}) \\ \epsilon_{j1}\epsilon_{j2} & \epsilon_{j1}\epsilon_{\gamma 2} & \epsilon_{\gamma 1}\epsilon_{j2} & \epsilon_{\gamma 1}\epsilon_{\gamma 2} \end{pmatrix}$$

- For instance, if leading passes/trailing fails, the event weight is:
- Estimated number of prompt diphoton events bin-by-bin is given by the sum of $\gamma\gamma$ weights:

$$N_{\gamma\gamma} = \sum_{i=1}^{N_{data}} w_{\gamma\gamma}^i$$



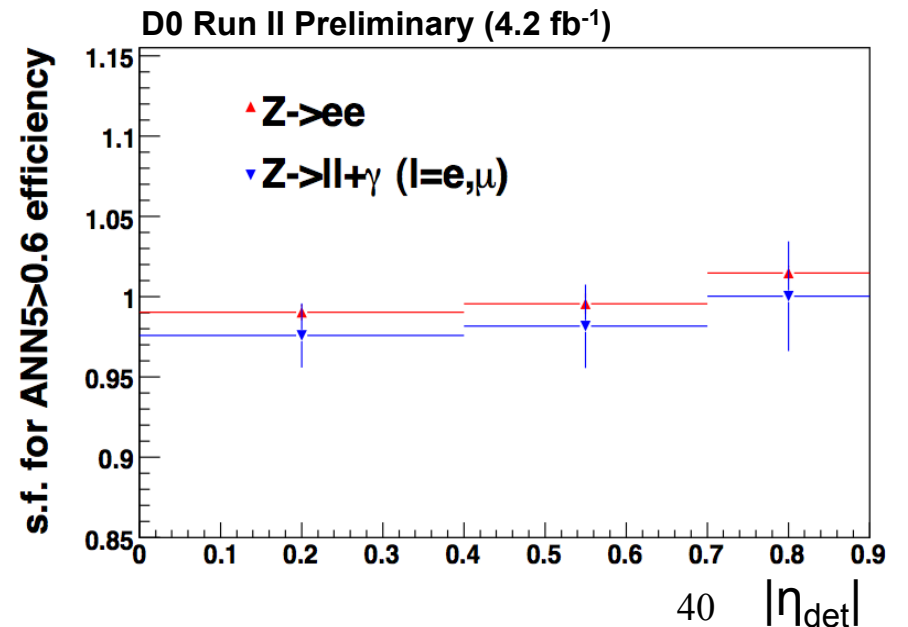
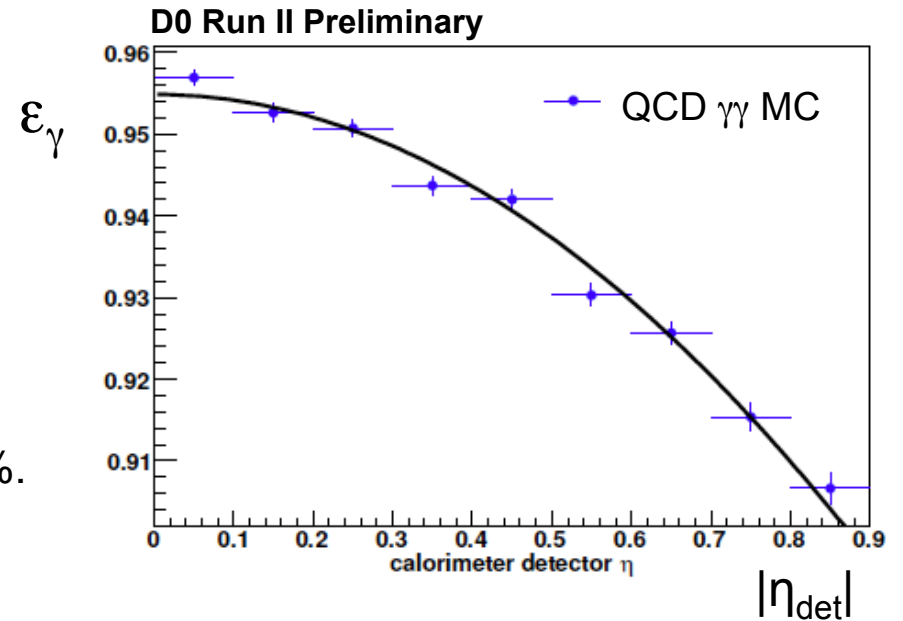
$$\begin{pmatrix} w_{ff} \\ w_{fp} \\ w_{pf} \\ w_{pp} \end{pmatrix} = \begin{pmatrix} 0 \\ 0 \\ 1 \\ 0 \end{pmatrix}$$

Background estimation: 4x4 Matrix Method

- Relative efficiencies for photon and jet estimated as a function of $|\eta_{\text{det}}|$ using MC.

Photon efficiency: $\epsilon_\gamma \sim 90\text{-}95\%$

- data-MC scale factor measured in $Z \rightarrow ee$ and $Z \rightarrow l^+l^-\gamma$.
- Small correction ($<2\%$) based on $Z \rightarrow ee$
- Scale factor for e and γ consistent within 1.5%.

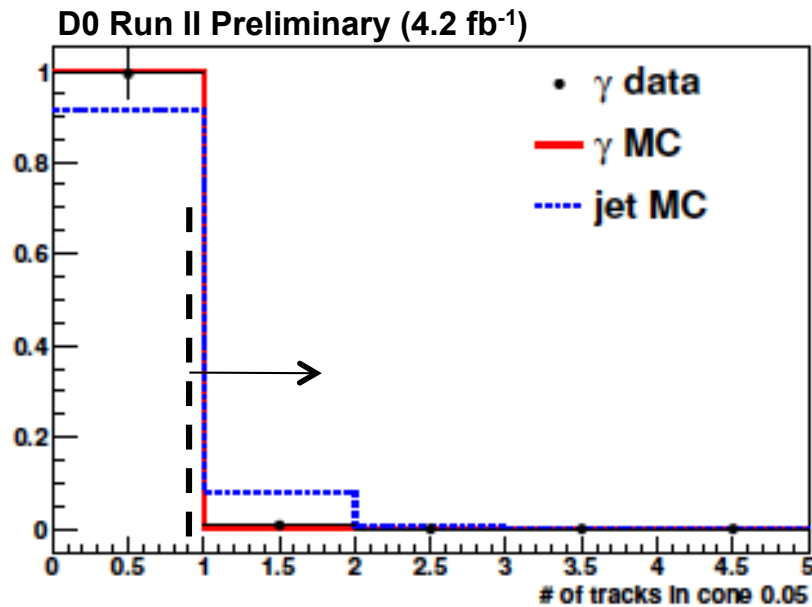
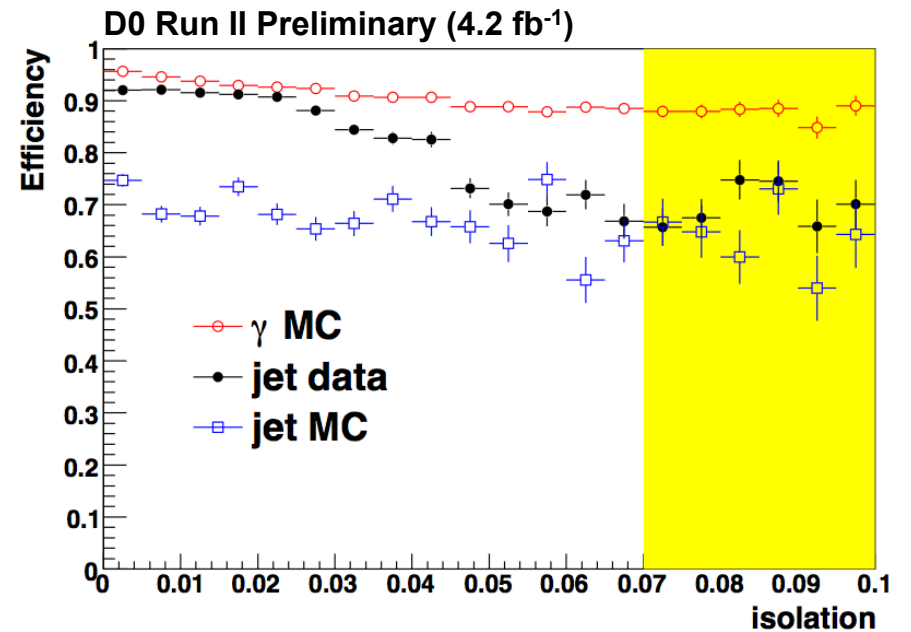


Background estimation: 4x4 Matrix Method

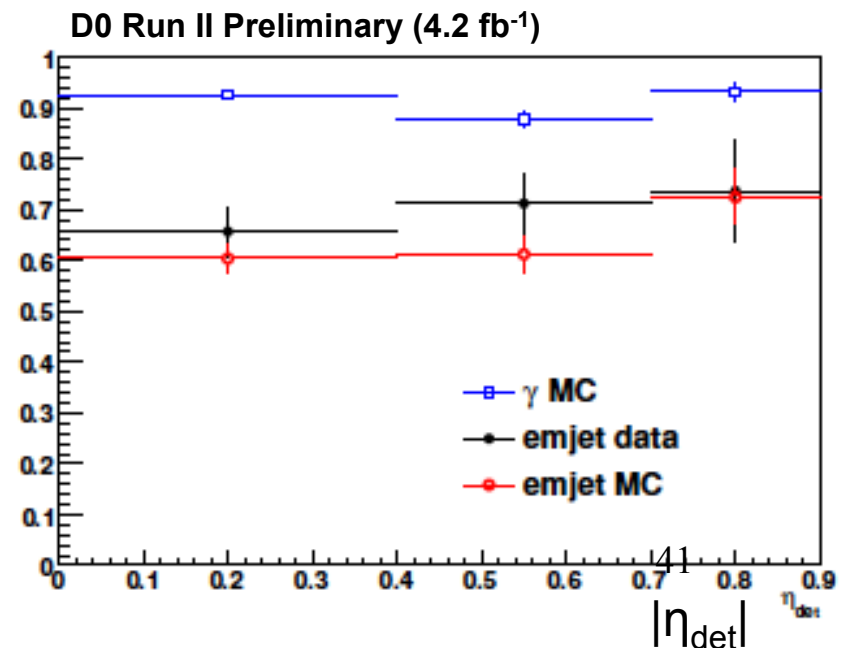
- Relative efficiencies for photon and jet estimated as a function of $|\eta_{\text{det}}|$ using MC.

Jet efficiency: $\epsilon_j \sim 68\%$

- compare data and MC in “sideband” regions:
- As a function of photon isolation.
- For photon candidates with tracks within $\Delta R < 0.05$.



→ Data and MC consistent to within 10%.

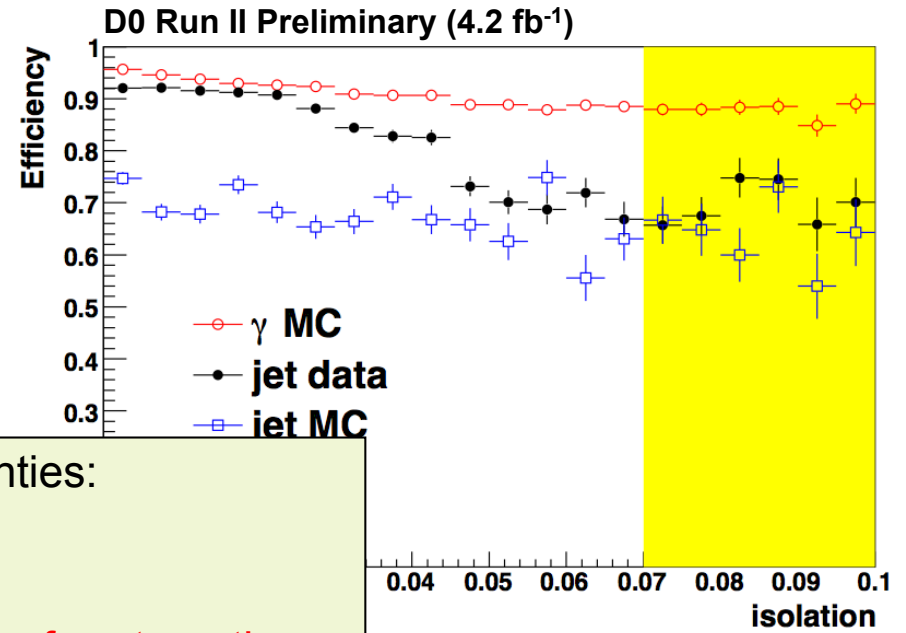


Background estimation: 4x4 Matrix Method

- Relative efficiencies for photon and jet estimated as a function of $|\eta_{\text{det}}|$ using MC.

Jet efficiency: $\epsilon_j \sim 68\%$

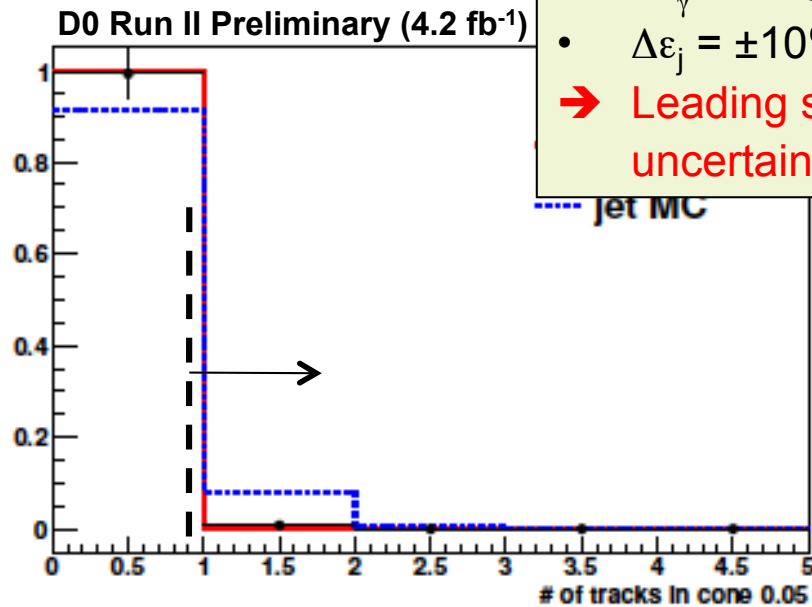
- compare data and MC in “sideband” regions:
- As a function of photon isolation.
- For photon candidates with tracks within $\Delta R < 0.05$.



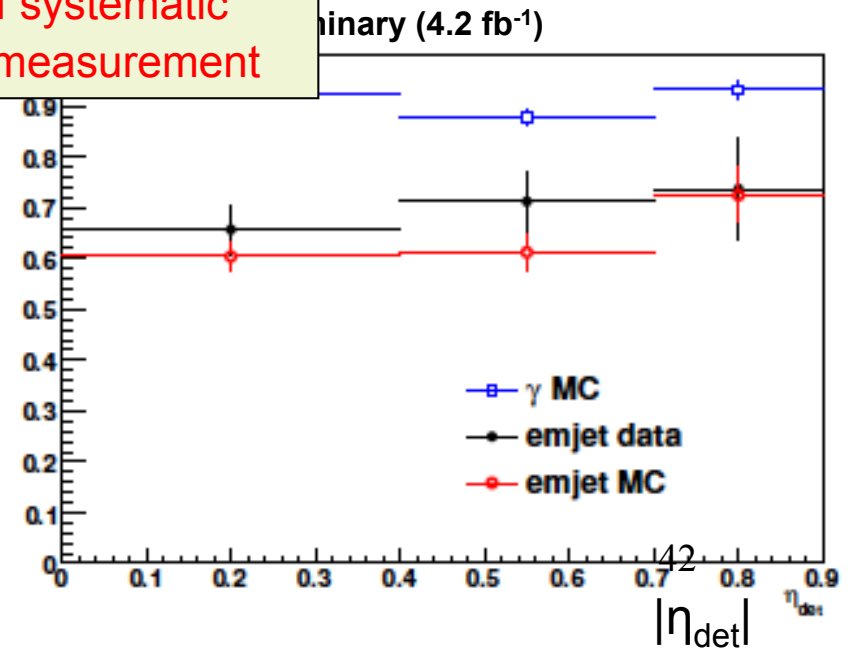
Systematic uncertainties:

- $\Delta\epsilon_\gamma = \pm 1.5\%$
- $\Delta\epsilon_j = \pm 10\%$

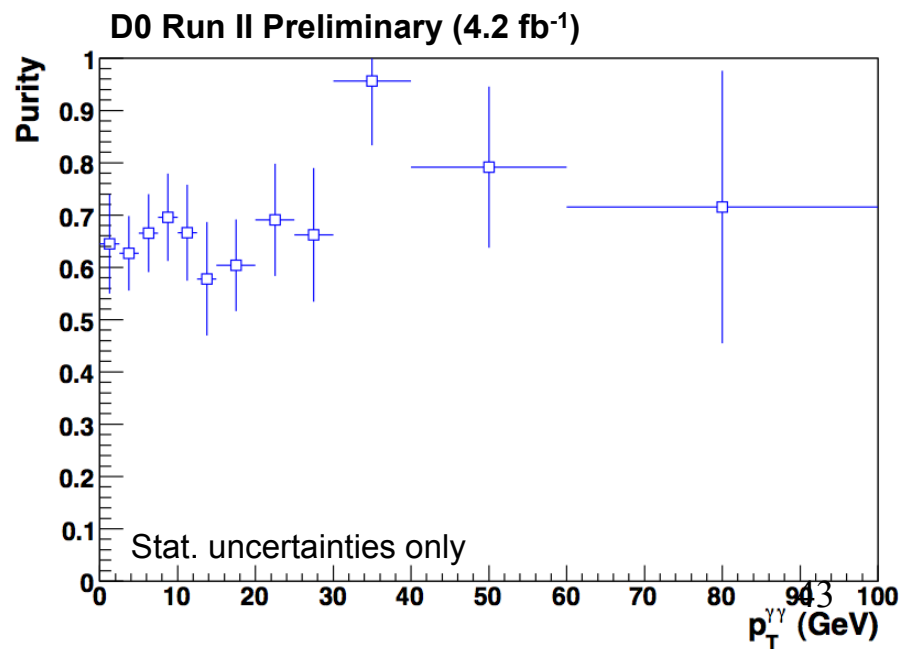
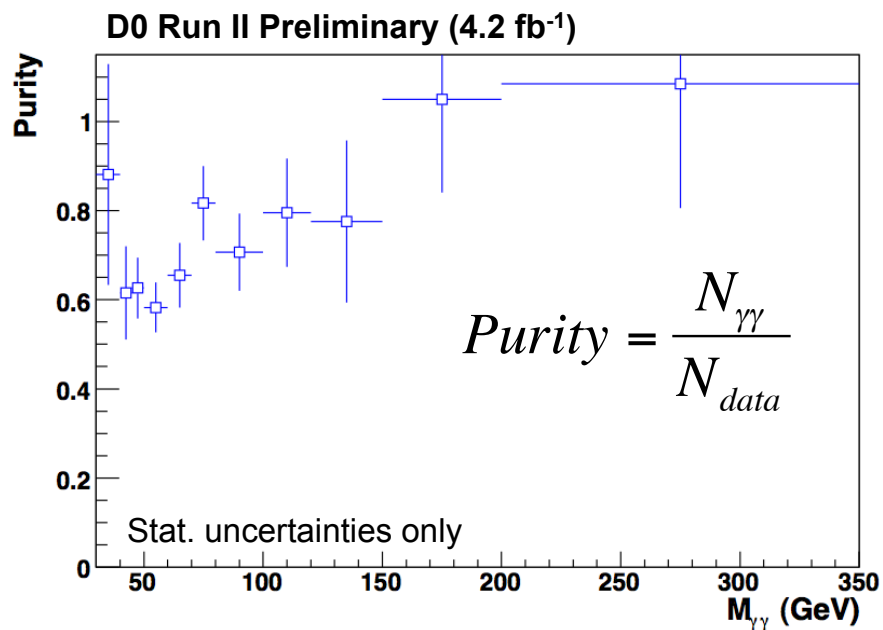
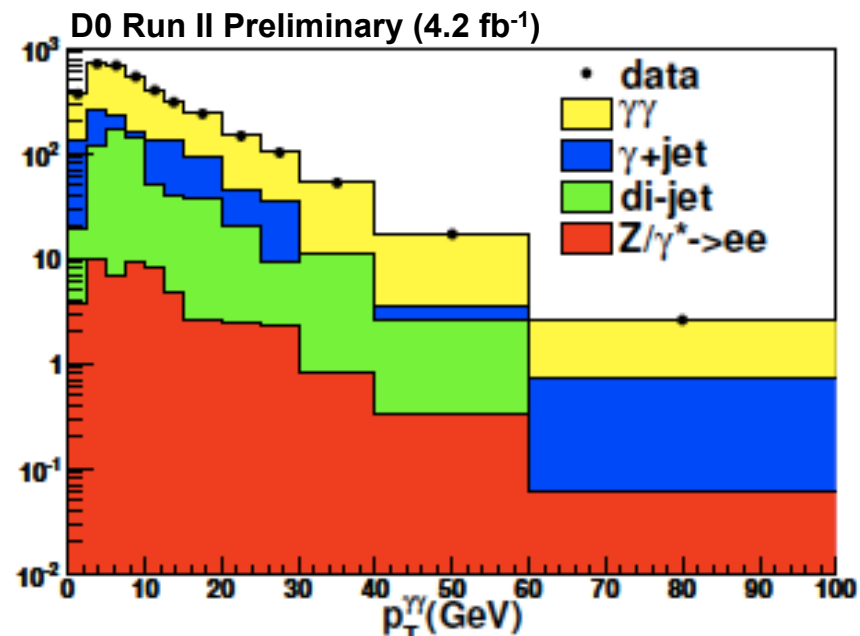
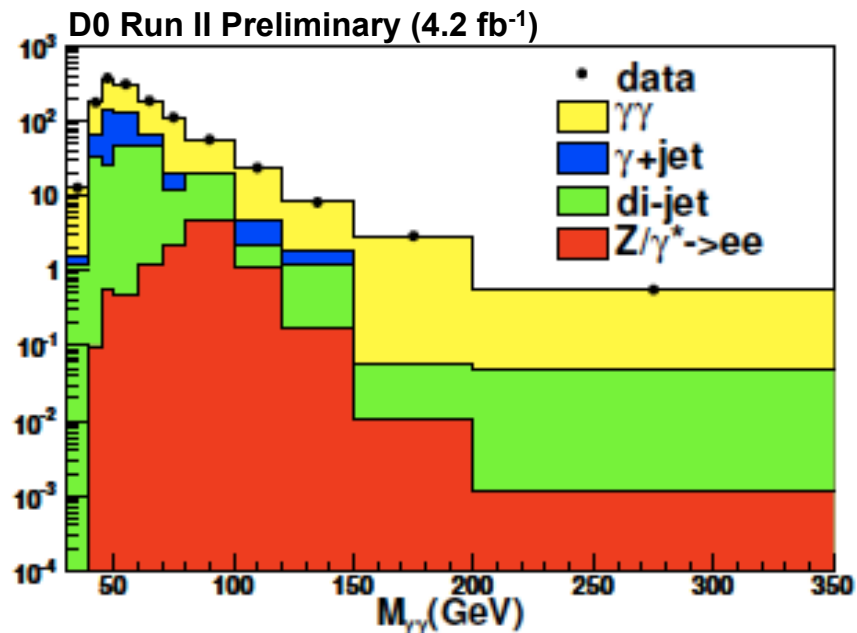
→ Leading sources of systematic uncertainty in this measurement



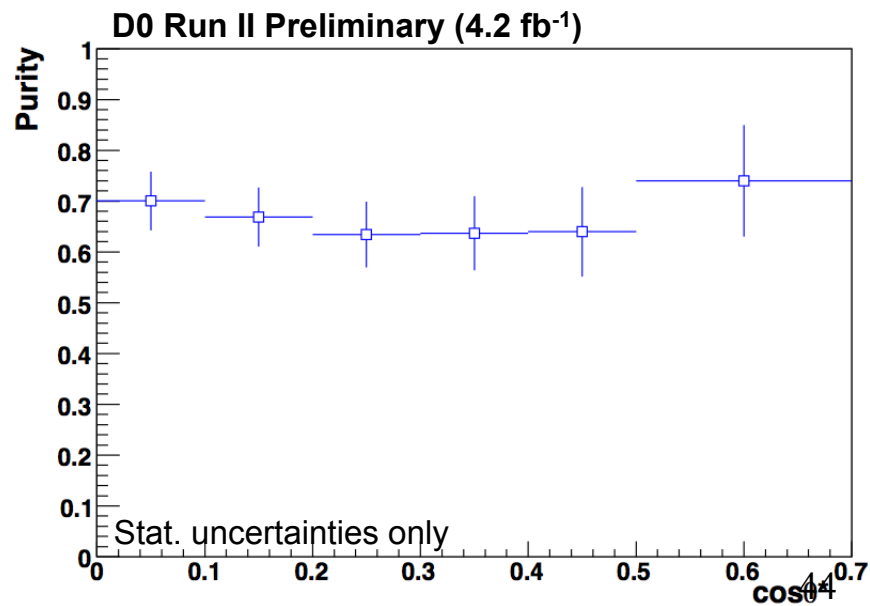
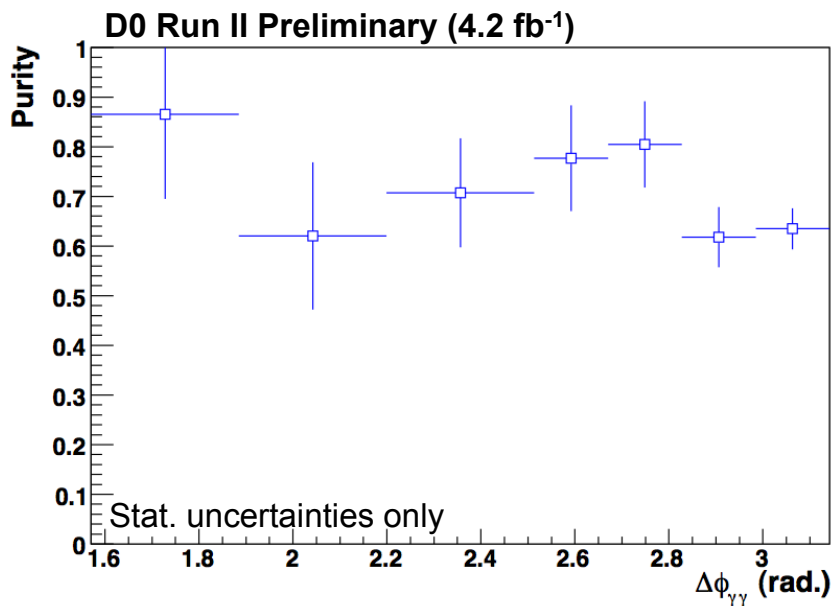
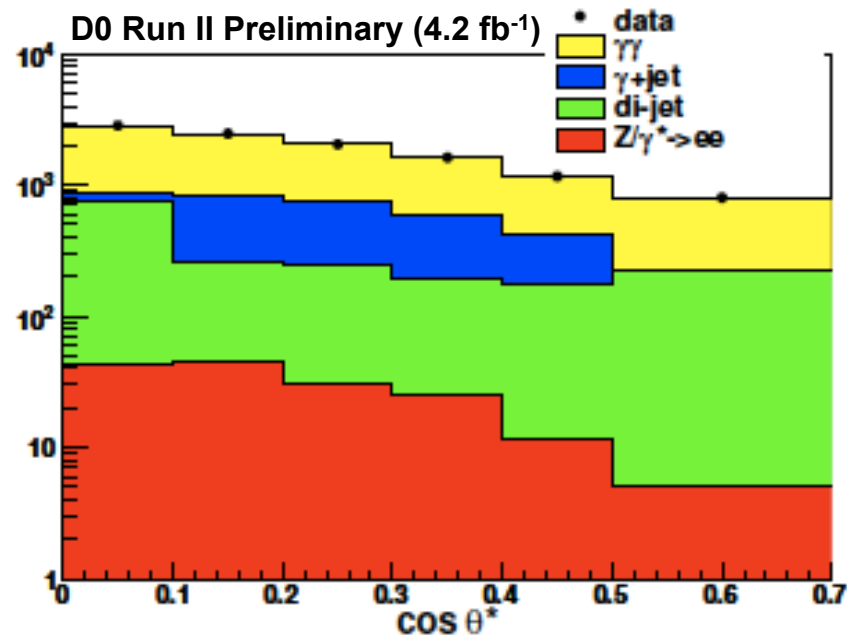
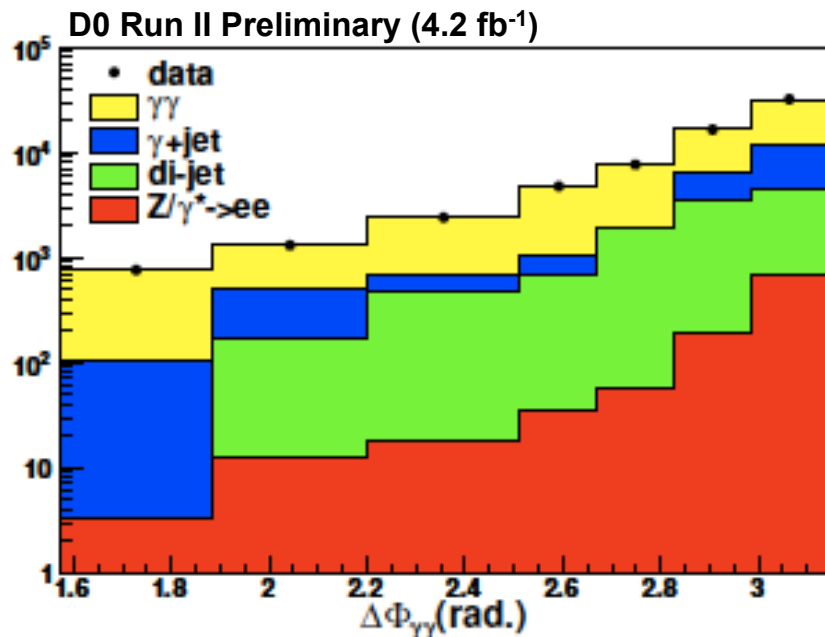
→ Data and MC consistent to within 10%.



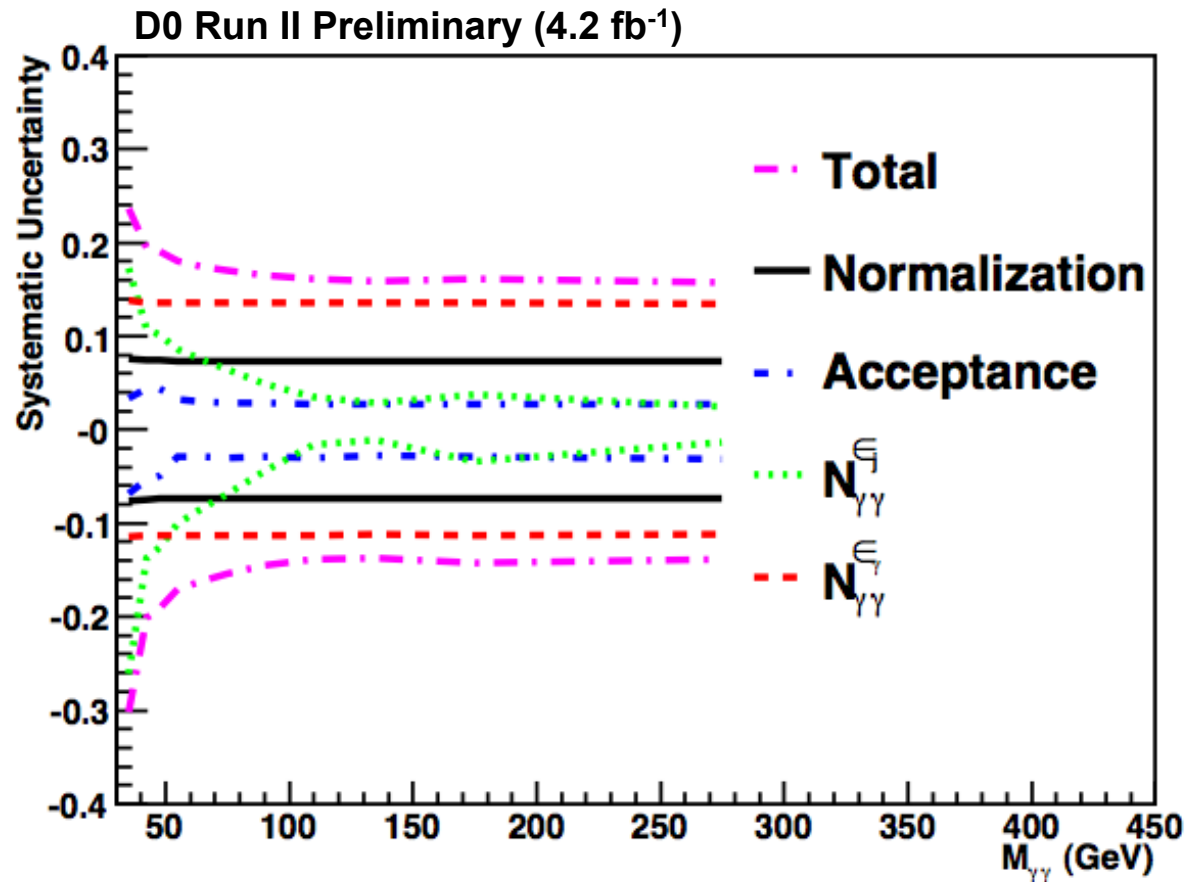
Estimated sample composition



Estimated sample composition



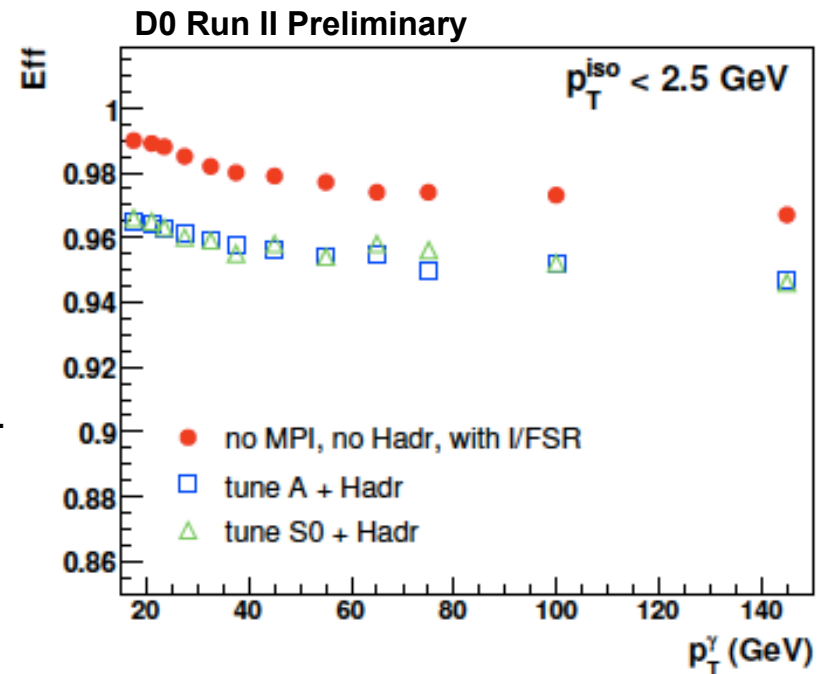
Experimental systematic uncertainties



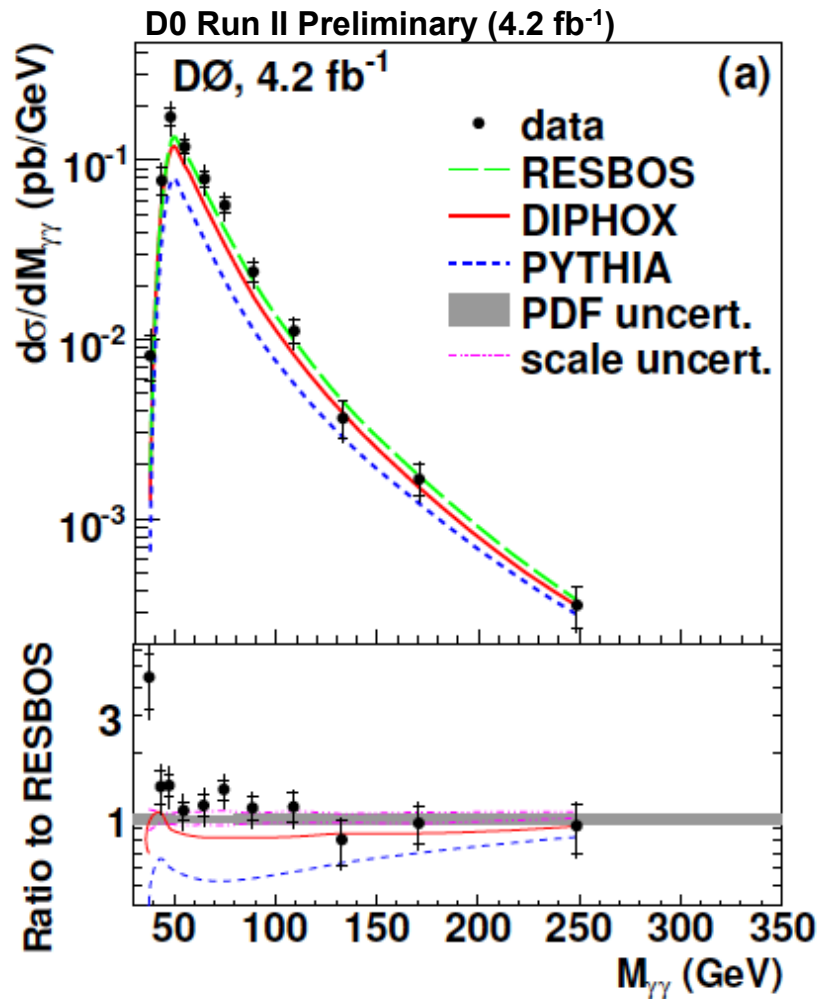
- Total systematic uncertainty $\sim 18\%$, rather flat as a function of the kinematic variables considered.
- Main source is diphoton purity, followed by overall normalization (selection efficiency: 4.1%; integrated luminosity: 6.1%).
- Full information on bin-to-bin correlations for each systematic uncertainty preserved.

Theoretical predictions

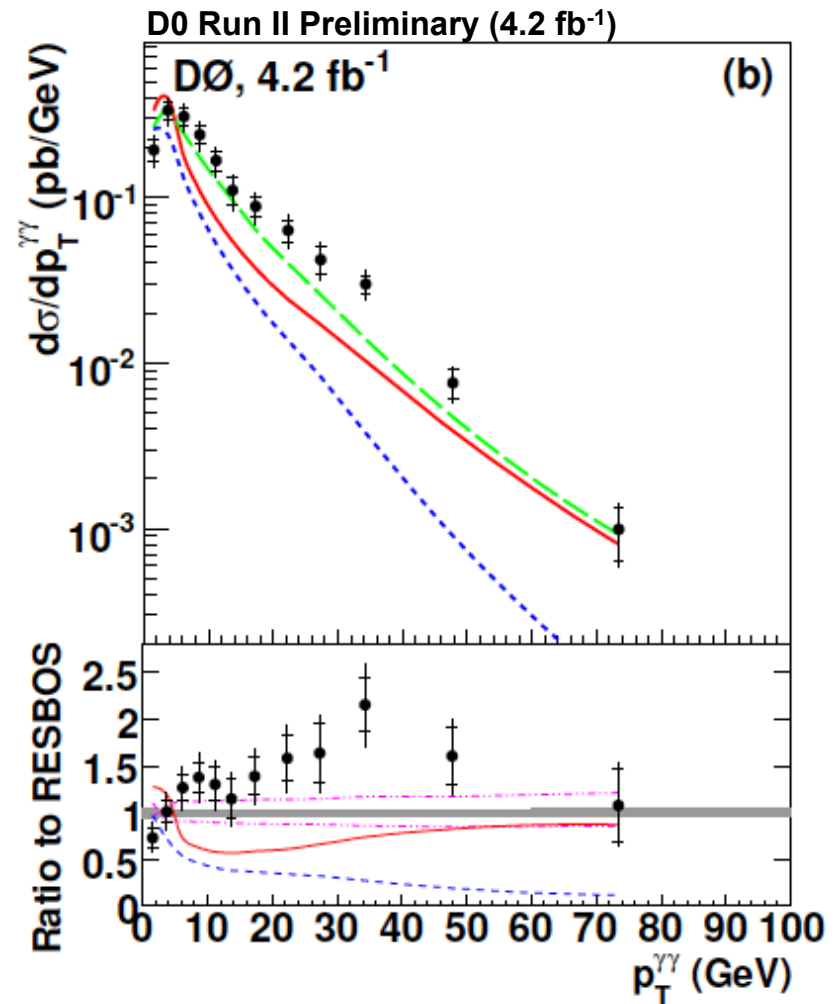
- RESBOS and DIPHOX use CTEQ6.6M PDFs and $\mu_R = \mu_F = \mu_f = M_{\gamma\gamma}$.
- PYTHIA v6.420 using Tune A (CTEQ5L).
- RESBOS and DIPHOX need to be corrected for non-perturbative effects: underlying event and hadronization
→ lower efficiency of the isolation cut.
- Correction estimated as a function of each observable using PYTHIA and considering two different underlying event tunes (Tune A and S0).
 - Total correction ~4-5.5%.
 - Both tunes consistent within 0.5%.
- Theoretical uncertainties:
 - PDFs: 3-6%; use 44 eigenvectors from CTE6.6M.
 - Renorm/fact/fragm scales: ~10-20% depending the observable; all scales simultaneously varied by x2 up and down.



Single-differential cross sections

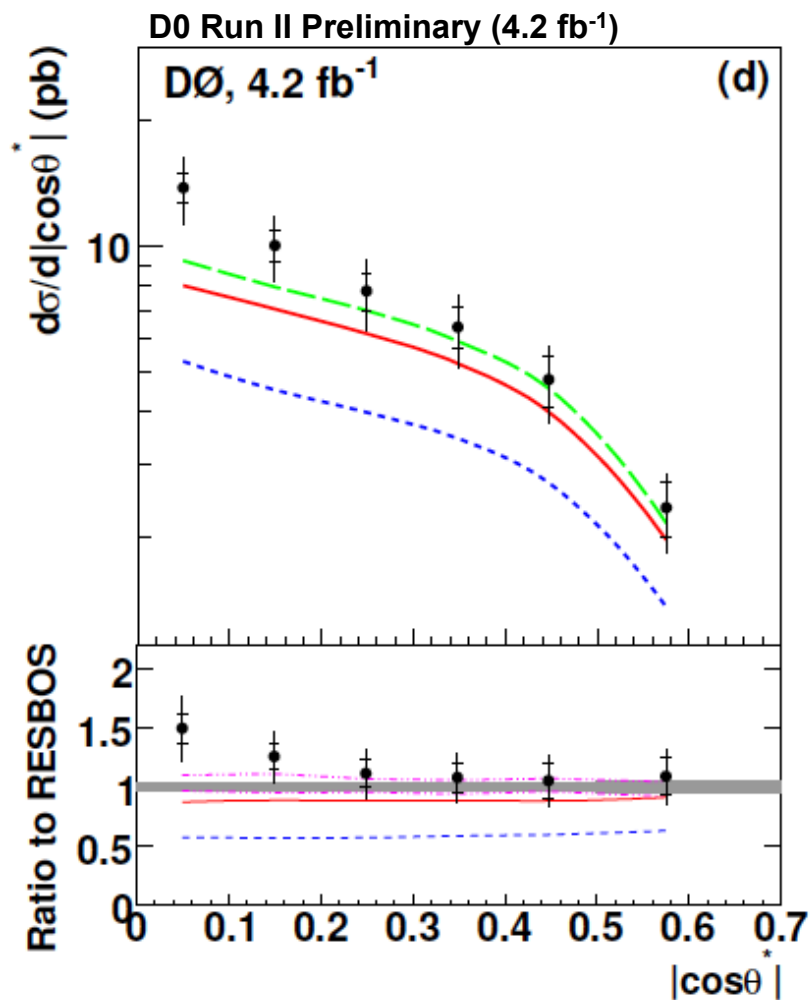
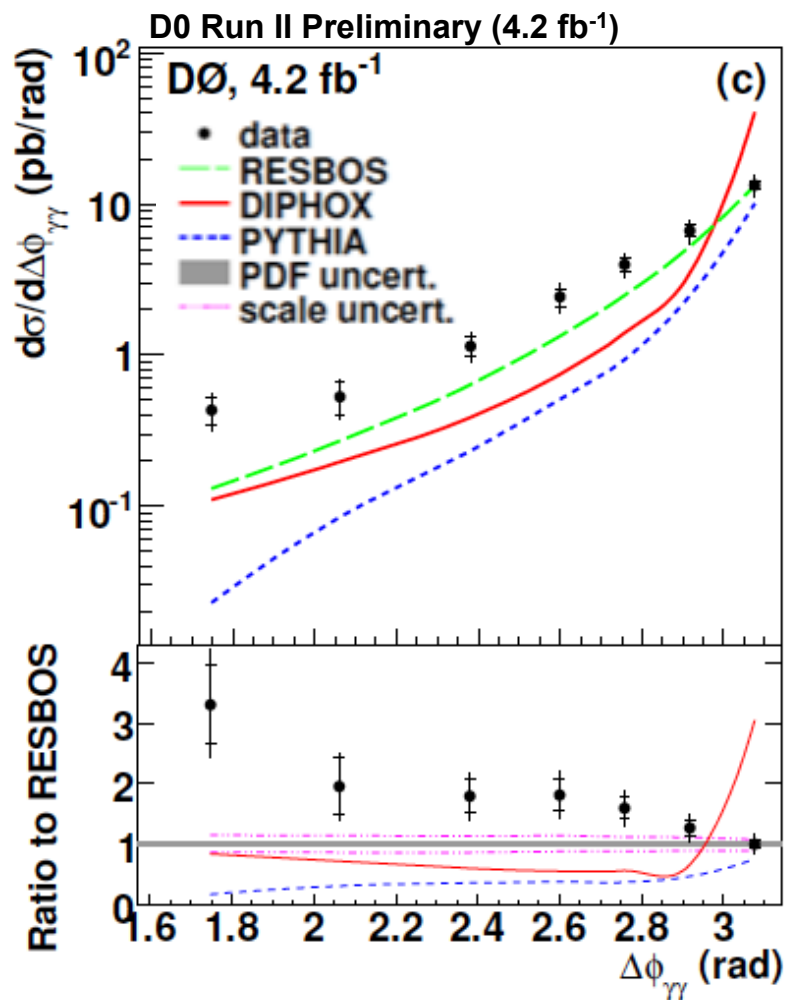


- Good agreement between data and RESBOS for $M_{\gamma\gamma} > 50$ GeV.



- Clear need for a resummed calculation. Data spectrum harder than predicted.

Single-differential cross sections



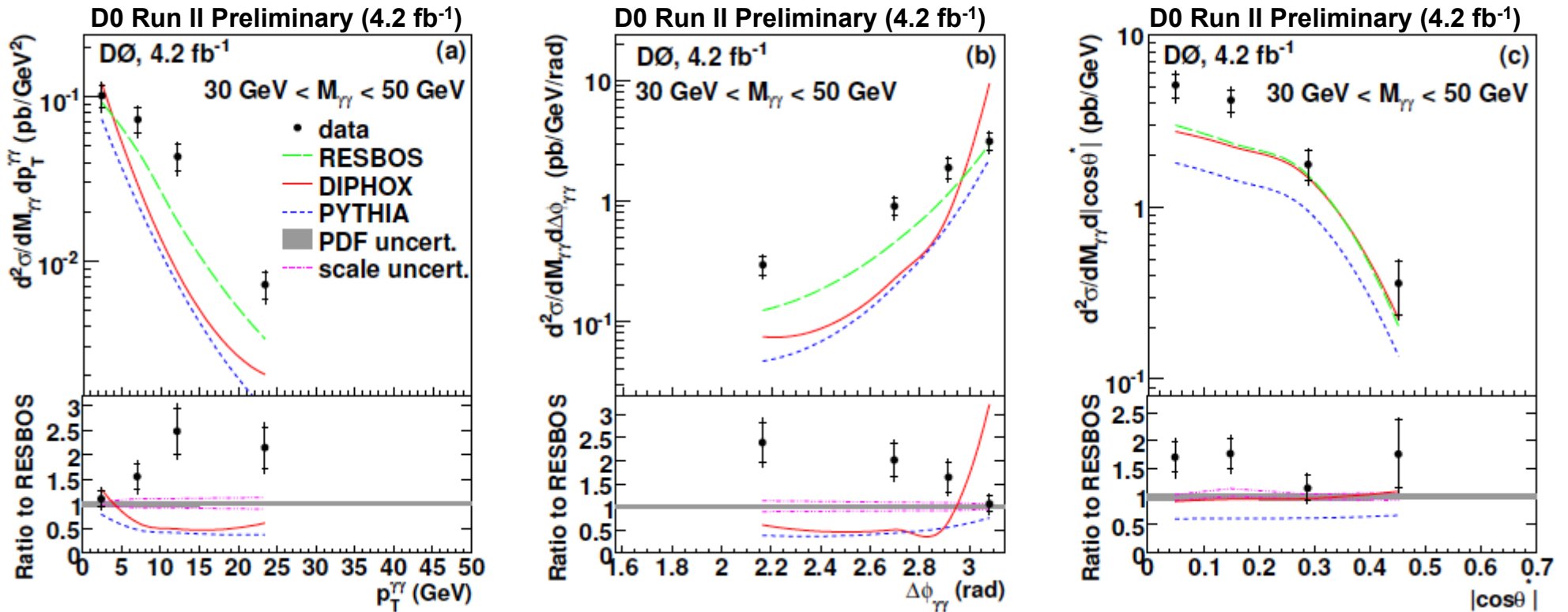
- Observable basically insensitive to experimental effects. Supports conclusion from $p_T(\gamma\gamma)$ measurement.

Further insight can be gained by examining double-differential cross sections.

(*) Overall normalization uncertainty (7.3%) not included in data error bars.

Double-differential cross sections

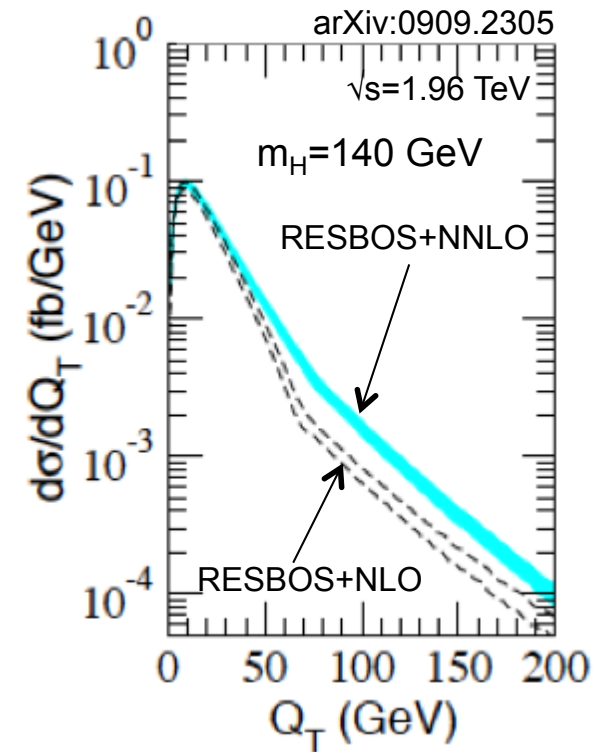
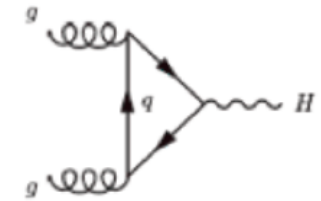
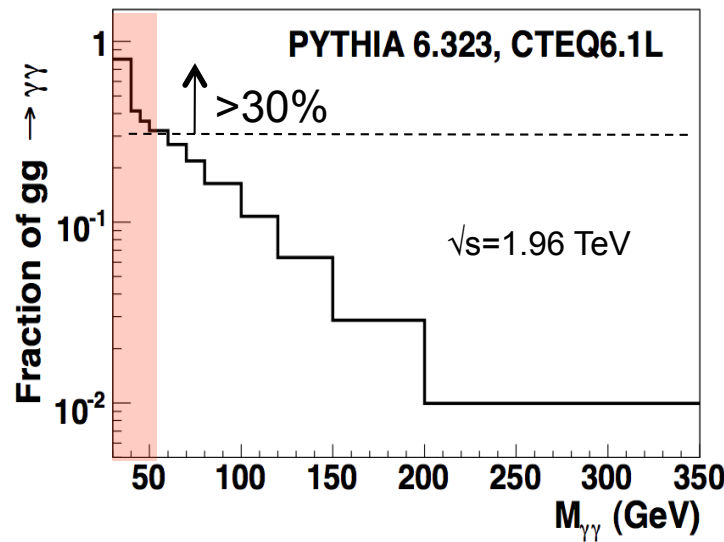
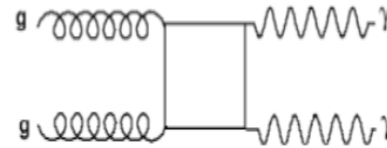
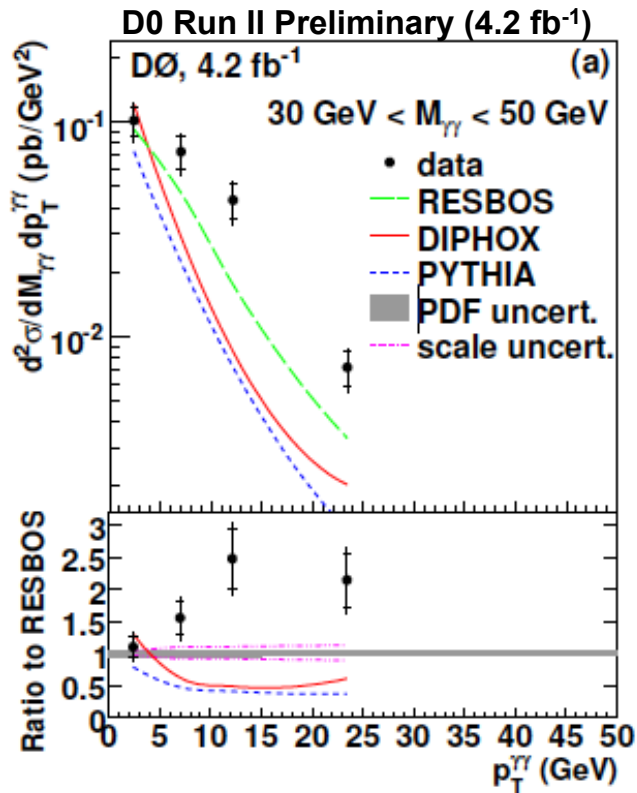
$$30 \leq M_{\gamma\gamma} < 50 \text{ GeV}$$



- RESBOS correctly predicts the rate for diphoton prediction at low p_T(γγ) (<5 GeV), but underestimates rate at higher p_{Tγγ} by up to a factor of ~2.

Double-differential cross sections

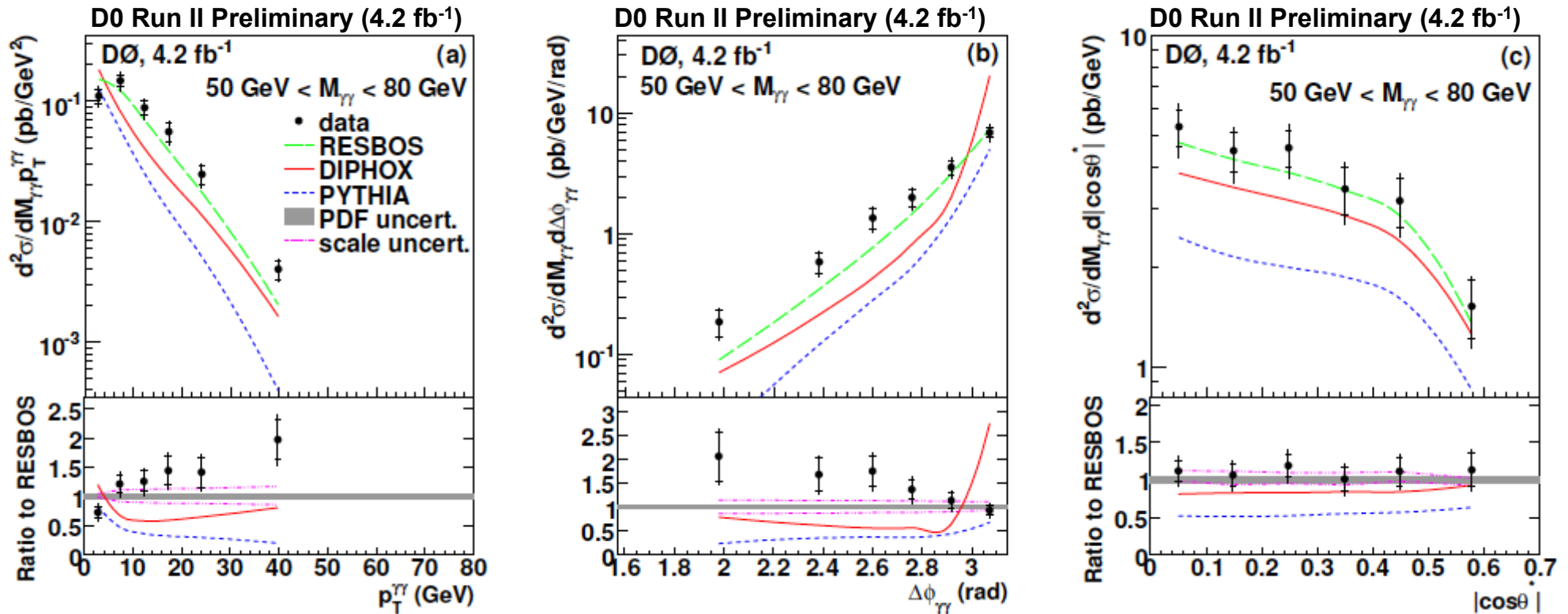
$$30 \leq M_{\gamma\gamma} < 50 \text{ GeV}$$



- This is the region where the gg process is dominant!
- Sizable NNLO effects were found in $gg \rightarrow H$ at a mass ~ 140 - 170 GeV. Potential for similarly large NNLO corrections at lower masses?

Double-differential cross sections

$$50 \leq M_{\gamma\gamma} < 80 \text{ GeV}$$

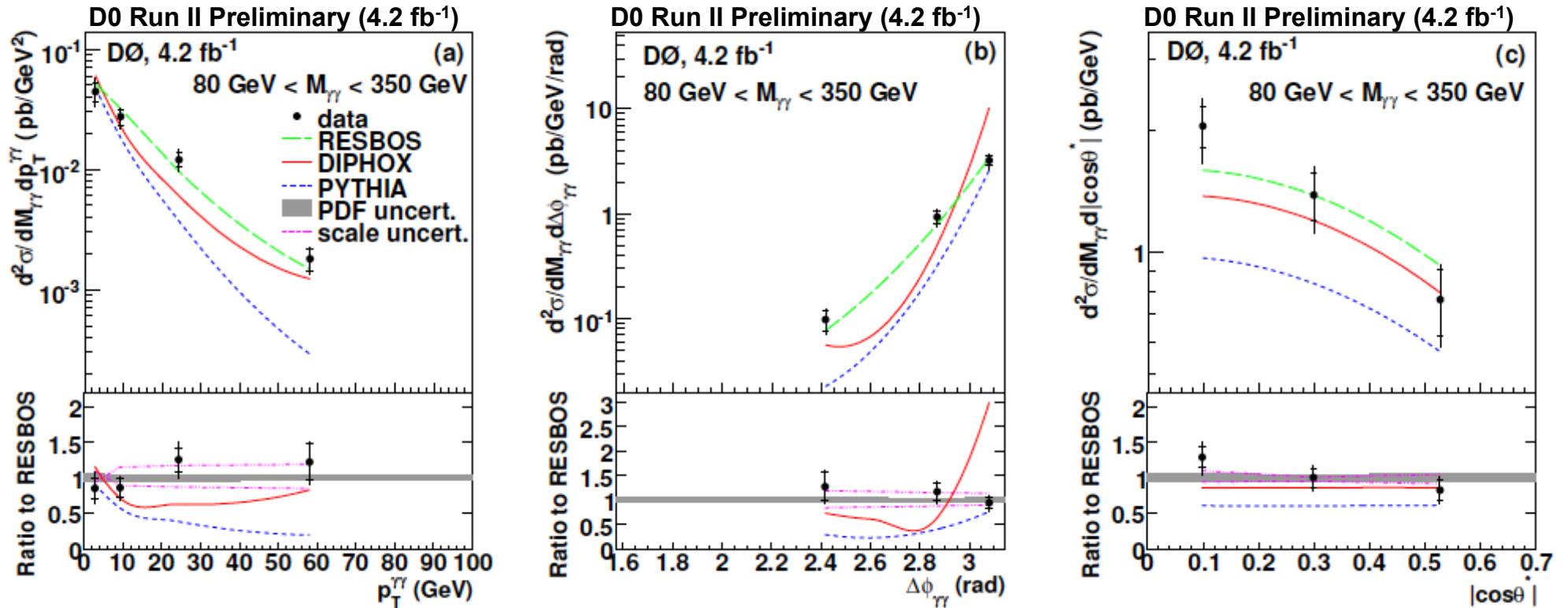


- Qualitatively same observations as in the 30-50 GeV mass bin, although overall agreement of RESBOS to data much improved.

(* Overall normalization uncertainty (7.3%) not included in data error bars.

Double-differential cross sections

$$80 \leq M_{\gamma\gamma} < 350 \text{ GeV}$$



- Excellent agreement between RESBOS and data in the kinematic region of most interest for Higgs and NP searches!

Summary and Conclusions

- We have presented measurements of single- and, for the first time, double-differential cross sections for direct diphoton production at $\sqrt{s}=1.96$ TeV using 4.2 fb^{-1} .

$$\begin{array}{cccc}
 \frac{d\sigma}{dM_{\gamma\gamma}} & \frac{d\sigma}{dp_T^{\gamma\gamma}} & \frac{d\sigma}{d\Delta\phi_{\gamma\gamma}} & \frac{d\sigma}{d|\cos\theta^*|} \\
 \\
 \frac{d^2\sigma}{dM_{\gamma\gamma} dp_T^{\gamma\gamma}} & \frac{d^2\sigma}{dM_{\gamma\gamma} d\Delta\phi_{\gamma\gamma}} & \frac{d^2\sigma}{dM_{\gamma\gamma} d|\cos\theta^*|} & \left\{ \begin{array}{l} 30 \leq M_{\gamma\gamma} < 50 \text{ GeV} \\ 50 \leq M_{\gamma\gamma} < 80 \text{ GeV} \\ 80 \leq M_{\gamma\gamma} < 350 \text{ GeV} \end{array} \right.
 \end{array}$$

- Our measurements are compared to state-of-art theoretical predictions such as DIPHOX and RESBOS, as well as PYTHIA. None of the theoretical predictions fully describes the data in all kinematic regions of the four variables considered.
- The best agreement is obtained for RESBOS, demonstrating the need to include corrections beyond NLO and resummation of soft/collinear gluons in the initial state. Excellent agreement in the kinematic region of most interest for Higgs and NP searches!
- These measurement should allow further refinements to the theoretical predictions.